SUPERBEND UPGRADE ON THE ADVANCED LIGHT SOURCE ⋆

D. Robin [a,*] J. Krupnick [a] R. Schlueter [a] C. Steier [a] S. Marks [a]

B. Wang [b] J. Zbasnik [a] R. Benjegerdes [a] A. Biocca [a] P. Bish [a]

W. Brown [a] W. Byrne [a] J. Chen [b] W. Decking [c] J. DeVries [a]

W. R. DeMarco [a] M.Fahmie [a] A. Geyer [a] J. Harkins [a]

T. Henderson [a] J. Hinkson [a] E.Hoyer [a] D. Hull [a] S. Jacobson [a]

J. McDonald [a] P. Molinari [a] R. Mueller [a] L. Nadolski [a]

H. Nishimura [a] K. Nishimura [a] F. Ottens [a] J.A. Paterson [a]

P. Pipersky [a] G. Portmann [a] A. Ritchie [a] S. Rossi [a] B. Salvant [a]

T. Scarvie [a] A. Schmidt [a] J. Spring [a] C. Taylor [a] W. Thur [a]

C. Timossi [a] A. Wandesforde [a]

[a] *LBNL, Berkeley, CA, USA 94720*

[b] *WANG NMR, Livermore, CA, USA 94550*

[c] *DESY, Hamburg, Germany*

Abstract

The Advanced Light Source (ALS) is a third generation synchrotron light source located at Lawrence Berkeley National Laboratory (LBNL). There was an increasing demand at the ALS for additional high brightness hard x-ray beamlines in the 7 to 40 keV range. In response to that demand, the ALS storage ring was modified in

August 2001. Three 1.3 Tesla normal conducting bending magnets were removed and replaced with three 5 Tesla superconducting magnets (Superbends). The radiation produced by these Superbends is an order of magnitude higher in photon brightness and flux at 12 keV than that of the 1.3 Tesla bends, making them excellent sources of hard x-rays for protein crystallography and other hard x-ray applications. At the same time the Superbends did not compromise the performance of the facility in the VUV and soft x-ray regions of the spectrum. The Superbends will eventually feed 12 new beam lines greatly enhancing the facility's capability and capacity in the hard x-ray region. The Superbend project is the biggest upgrade to the ALS storage ring since it was commissioned in 1993. In this paper we present an overview of the Superbend project, its challenges and the resulting impact on the ALS.

Key words: storage rings, superconducting, magnets, x-rays, beam dynamics
PACS: 29.20.Dh 29.27.Bd 84.71.Ba

1 Introduction

The Advanced Light Source (ALS) is a third generation synchrotron light source located at Lawrence Berkeley National Laboratory (LBNL) [24]. The ALS has been in operation since 1993 and it produces radiation from the IR to the hard x-ray region of the spectrum. The ALS has a large and diverse user community. The number of annual users has steadily grown over the years and in year 2004 the number of users is expected to be about 2000.

⋆ This work was supported by the Director, Office of Energy Research, Office of Basic Energy Sciences, Materials Sciences Division of the U.S. Department of Energy, under Contract No. DE-AC03-76SF00098.

* corresponding author
Email address: dsrobin@lbl.gov (D. Robin).

The ALS was initially designed to be optimized for the generation of radiation from the VUV to Soft x-ray range (10 to 1500 eV). In this spectral region (considered the core region of the ALS) the ALS is one of the brightest sources of radiation in the world. Over the years the ALS has developed a strong user community in this core region. At the same time, the ALS saw a large growth in user communities outside of this core region — particularly in the hard x-ray region.

Prior to the installation of the Superbends there were two sources of hard x-rays: normal conducting 1.3 Tesla dipoles and a 2.1 Tesla wiggler. The beamline which uses 12 keV photons generated from the wiggler proved to be one of the most productive protein crystallography beamlines in the world demonstrating the capabilities of lower electron energy synchrotrons like the ALS to do hard x-ray science [6]. The success of the initial wiggler beamline together with the need for more protein crystallography beamlines worldwide [7] fueled the demand for more hard x-ray beamlines at the ALS. There was also a demand from the tomography and powder diffraction communities demanding even higher energy x-rays (up to 40 keV). Due to this demand for more hard x-ray sources, there was a strong incentive to include more hard x-ray sources in the storage ring.

To better serve this demand, the Superbend project was formed with the objective to significantly enhance the capability and capacity of the ALS in the hard x-ray regime while not compromising the performance of the ALS in the VUV and soft x-ray region. The basic idea behind the Superbend project was to replace three lower field (1.3 Tesla) normal conducting magnets with three high field (5 Tesla) magnets. For the ALS the Superbends offered many advantages over other sources of hard x-rays.

1.1 Superbends versus Wigglers

There are several types of synchrotron based sources for generating hard x-rays — bending magnets, wigglers, or undulators. Due to the relatively low electron beam energy, 1.9 GeV, of the ALS the generation of 12 - 40 keV photons was impractical with an undulator at time the Superbend project started. Therefore the practical choices were bends or wigglers. At an electron beam energy of 1.9 GeV and a Superbend field of 5 Tesla, the Superbend beamlines have a critical photon energy of 12 keV and are a good source of photons up to 40 keV (see Fig. 1).

In principle the ALS could have chosen to use wigglers to generate hard x-rays. However, for the ALS, the Superbend solution was superior. First, by replacing normal bends with Superbends, none of the few remaining empty insertion device straight sections were used. Second, the Superbends provided high capacity—up to 12 new beamlines (four from each bend) versus a wiggler that only can support 3 beamlines. Third, on most of the Superbend beamlines, the powerful technique of multiple-wavelength anomalous diffraction (MAD) can be used whereas only the central beamline and not the side stations on the wiggler is capable of using MAD. Fourth, the Superbends were higher in flux density than the wiggler (due to the smaller electron beam size) making them a superior source of 12 keV photons for protein crystallography [3,5]. This meant that the experimental beam time is shorter. Fifth, the total radiation power in the Superbend beamlines is significantly smaller than that of the wiggler making the beamlines simpler. All totaled, the Superbend solution was a cost effective way to greatly increase the hard x-ray capability of the ALS facility.

1.2 History

The idea of retrofitting the ALS storage ring with high field superconducting magnets to produce hard x-rays was conceived in the early 1990s. In 1995 a project began to see if it was possible to design a superconducting coil and core of a magnet that would meet the needs of the ALS [8]. In 1998, based upon the successful tests of a coil and core [9] combined with the increasing demand from the user community, the ALS decided to embark upon the Superbend project [2,6]. The project began in September 1998 and concluded three years later. October 4, 2001 marked the completion of the Superbend Project. On that day, the ALS facility began user operation with three newly installed Superbends and first light generated from one of these Superbends reached the end station of the first Superbend beamline. With the successful completion of the Superbend project the ALS has transformed itself, greatly increasing its capability and capacity to deliver bright hard x-ray beams (up to 40 keV) to users [1–4].

1.3 Structure of the Paper

In Section 2 we discuss project goal and challenges. In addition, details of the lattice modifications will be discussed. In Section 3 we discuss the Superbend magnet system. The requirements, design and performance tests of the various Superbend components will be discussed. In Section 4 we discuss the precommissioning studies. In particular we discuss tests of systems other than the Superbend magnets as well as nonlinear beam dynamics studies. In Section 5 we discuss the installation and commissioning of the Superbends. In

Section 6 we discuss the operational experience of the ALS with Superbends. In Section 7 we conclude with some summary remarks about the impact of the Superbend upgrade on the ALS.

2 Project Goals and Challenges

2.1 ALS Lattice Modifications

To include the Superbends it was necessary to modify the storage ring magnetic lattice. Fig. 2 shows a clock diagram of the ALS with its beamlines. The ALS lattice is built up of twelve sectors. As part of the Superbend project 3 of the 12 sectors in the the storage ring lattice were modified by replacing 3 of the 36, 1.3 Tesla, normal conducting, 10 degree, bending magnets with three, 5 Tesla, superconducting, 10 degree, bending magnets (Superbends) [10,14]. The modified sectors were 4, 8, and 12 as shown in green in Fig 2.

The Superbend reaches a peak magnetic field of 5.7 Tesla and is about 5 Tesla at the locations of the four beamlines. Fig. 3 shows how each of the 3 sectors was modified to include Superbends. A typical sector without Superbends can be seen in Fig. 3 (top) and one modified to include Superbends is shown in Fig. 3 (bottom). One sees that the central dipole in the sector is replaced by a Superbend.

Unlike the normal dipoles, the Superbends do not have a quadrupole focusing component. Two new quadrupoles QDA1 and QDA2 are added to the lattice and the QFA quadrupoles in a Superbend sector are put on separate power supplies. It was necessary to make this change in the quadrupole configuration

in order to better match the Superbend sectors to the non Superbend sectors to minimize the impact on the particle beam dynamics. In addition the modified sectors (4, 8, and 12) were chosen to be symmetrically located around the storage ring in order to maximize the lattice periodicity [25]. The importance of the lattice periodicity is discussed in subsection 4.1. Specifically sectors 4, 8, and 12 were chosen because there were no previously installed beamlines in the center bends of those sectors.

2.2 Challenges

Choosing Superbends as a source of hard x-rays left the ALS with some unique challenges. The Superbends would be an integral part of the storage ring lattice and problems with them not only affect the users of the Superbends, but all users at the ALS. This is different from insertion devices where turning off the device only affects the users of insertion device beamline. Therefore it was necessary to ensure that the transition to Superbend operation was transparent. Since the ALS is an operating user facility it is important the minimize the downtime. Typically there is only one shutdown per year lasting about 6 weeks. The Superbends needed to be installed and commissioned in a short period. After the installation and commissioning of the Superbends were finished the resulting influence on the existing users should be small. For these users there could be no significant impact on brightness, fill times, lifetime, beam orbit stability, or reliability.

In terms of brightness, the biggest concern was that the higher fields of the Superbends would increase the horizontal emittance and reduce the photon brightness. Prior to the installation of the Superbends, the horizontal emit-

tance at 1.9 GeV was 5.5 nm rad. At that time, the lattice of the ALS was adjusted to have zero dispersion in the insertion device straight sections. The lattice functions before Superbends can be seen in Fig. 4. Including Superbends in the lattice while keeping the dispersion adjusted to zero in the straights would more than double the emittance. Fortunately it was possible to reduce the horizontal emittance by adjusting the lattice to have slightly positive horizontal dispersion in the straights. For instance adjusting the lattice to 6 cm of dispersion (see Fig. 5) would result in an horizontal emittance with Superbends that was just slightly higher ($\approx 20\%$) than before (6.75 nm rad). This minimuzed the impact on performance of the non Superbend beamlines. It was important to experimentally test the non zero dispersion lattice to see if it was possible to obtain the reduced emittance.

Fill times is another important performance criteria for the users. The ALS did not have a full energy injector and therefore before filling the storage ring the electron energy needs to be ramped from 1.9 GeV down to 1.5 GeV where the ring is filled and then ramped back up to 1.9 GeV. The full fill cycle is outlined in Fig. 6. The two areas of concern were the impact of Superbends on the energy ramping rate and the injection efficiency. Prior to the Superbend upgrade the ramping time was approximately 2 minutes in each direction. Therefore the design goal for the Superbend cryosystem was to allow ramping within a similar time. The power supply and control system for Superbends needed to coordinate well with the other magnets to minimally distort the beam orbit during ramping. In addition it was necessary to measure and understand the hysterises of the field versus current of the Superbends.

The impact of the lattice changes on the beam dynamics was of major concern for both injection and lifetime. As compared with the pre Superbend

lattice there were two qualitive differences. The sextupole strengths are (30%) larger in the Superbend lattice mostly resulting from smaller dispersion at the sextupoles in the nonzero dispersion lattice. Also including the Superbends reduced the periodicity of the lattice from twelve-fold to three-fold. The concern was that these changes would reduce the dynamic aperture [21,25] and momentum aperture [22].

In terms of fill rate the concern was the impact of the Superbend lattice on the dynamic aperture. In the ALS beam is injected into the storage ring displaced by approximately 10 mm inward from the stored beam. Prior to Superbends the dynamic aperture of the ALS was about 12 mm. It was necessary to ensure that the on-energy dynamic aperture was sufficiently large to accept the injected beam.

The lifetime of the ALS is mostly limited by Touschek lifetime. The main concern about lifetime was the possible reduction in the momentum aperture. In particular the concern was that the periodicity breaking of the lattice would also impact the off-energy dynamics.

Beam orbit stability is one of the most critical performance parameters for the users. Before Superbends, the ALS integrated rms orbit stability in the insertion device straights was about 3 μm horizontally and 2 μm vertically for a frequency range of 0.1 - 200 Hz. This can be compared with the rms beam-sizes of 250 μm horizontally and 30 μm vertically. There were two concerns about Superbend operation affecting the orbit stability. The first concern was that vibration of the Superbend cryosystem would cause the Superbends and neighboring magnets to vibrate thus creating orbit jitter. The second concern was power supply jitter of the normal and Superbends would generate orbit

jitter. Prior to installation of the Superbends all 36 normal conducting bends were powered by one power supply. In that case power supply fluctuations resulted in beam energy changes but not orbit changes. After the installation of Superbends, power supply fluctuations could cause both energy and orbit changes. Therefore both the tolerances of the cryosystem and bend magnet and Superbend power supplies were very tight.

Reliability or availability was another important performance criteria for the users. The Superbends could not significantly impact the total unscheduled downtime of the accelerator. Prior to the installation of the Superbends the availability defined as the percentage of delivered beam versus scheduled beam was greater than 95%. Therefore acceptable accumulated downtime of the machine as a function of Superbend systems had to be small — less than 1%.

3 SUPERBEND MAGNET SYSTEM

Ensuring a smooth transition and reliable operation posed many design challenges for the Superbend magnet systems. In particular the goal of a cost effective yet reliable system strongly impacted the design of the cryogenic systems [10,14–17]. Also each of the subsystems and finally the complete systems were thoroughly tested prior to the Superbend shutdown. In this section we discuss the requirements, design, and performance tests of the Superbend systems.

Beginning in 1995, a study [8] was commissioned to consider ways of increasing the photon energy in the ALS using superconducting dipole magnets. An R&D program was then carried out which culminated in a successful magnet that

did not quench before reaching critical current. It could be ramped in less than 100 s while submerged in liquid helium and had acceptable field quality [9]. This magnet was used as the starting point for the design and fabrication of the Superbend magnet system suitable for installation into the ALS. The detailed design and fabrication were completed by LBNL and Wang NMR.

3.1 System Requirements

The detailed magnetic requirements are contained in [11,10]. Several of the important requirements are listed in Table 1 and are derived from accelerator physics considerations. The first two requirements in Table 1 on integrated and peak fields were derived from the requirements that when operating at 1.9 GeV, the Superbends should provide a total bending angle of 10 degrees while maintaining a field of approximately 5 Telsa at the beam ports (located at angles of 1.95, 3.20, 6.75, and 8.00 degrees).

The requirements on multipole components of sextupole and higher were derived from particle tracking studies. Initially there was a fear that higher order multipole components might impact the injection efficiency and lifetime by reducing the dynamic aperture and momentum aperture. Of particular concern was the effect of a large systematic sextupole component that resulted from the shape of the pole (shown in Fig. 7). In the earlier R & D phase of the project, there were considerable discussions about the magnet pole shape. A more circular pole shape would be easier to wind tightly but would result in a large sextupole component as compared with a more rectangular pole shape. The resulting shape was a compromise and resulted in an integrated sextupole component of about half that of the main chromaticity compensating

sextupoles of the ALS.

The effect of the sextupole and higher order multipoles was studied by including both systematic and random multipole errors in tracking studies. These studies concluded that it was possible to include a rather large sextupole and higher order multipole fields in the Superbends without significantly impacting the dynamics. The reason is that the Superbends were located at the center of the triple bend achromat (see Fig. 5)where the β-functions are small in both the horzontal and vertical planes (0.95 m horizontally and 1.5 m vertically). Tracking studies also showed that if the Superbends were located in the outer bends of the sector where the vertical β-function is about 20 m, the systematic sextupole of the chosen design would significantly reduce the injection efficiency and lifetime.

The tolerances on absolute alignment shown in Table 1 are derived from the following considerations. The tolerance on longitudial position and roll were derived by restricting the allowable horizontal and vertical orbit errors (in the straights) to 2 and 0.2 μm respectively. The tolerances on horizontal position and vertical position were derived by restricting the allowable vertical β-beating and coupling respectively to less than 5%.

In Table 1, the tolerances on longitudinal and horizontal vibration were established to restrict the fast horizontal orbit jitter and the tolerances on vertical magnet vibration and rolling motion were established to restrict the fast vertical orbit jitter. The tolerances on field ripple were established to contain the fast horizontal orbit motion. The goal was to limit the contribution of the Superbends to the fast orbit motion to < 1 μm.

3.2 Superbend Design

In this section we discuss the design of the various Superbend components. In particular we will discuss the coil, cold mass, supports, cryogenic, power supply, and quench protection systems.

3.2.1 Coil and Cold Mass Design

R&D studies were performed for possible conductors of the Superbends [9] and the chosen conductor was supplied by Outokumpu. Its parameters are listed in Table 2.

The magnet was chosen to be C-shaped to allow it to be inserted into (or removed from) the storage ring without disassembling the vacuum chamber. Fig. 8 shows the exterior configuration of the Superbends. The Superbend configuration was chosen to be mostly compatible with existing ALS storage ring components such as electron beam vacuum chamber, vacuum valves, photon stops and the tunnel shielding walls. Nevertheless two modifications needed to be made to the existing infrastructure to accomodate the Superbends — the roof block shielding needed to be modified in order to provide more space for the cryogenic system. Also the outer portion of the vacuum chamber needed to be machined. These modifications will be discussed later.

The outer portion of the Superbend system is at room temperature. The cold mass assembly is mechanically connected to the room temperature outer portion via epoxy-fiberglass suspension straps with intermediate 50 K heat stations. Fig. 9 shows the essential features of the Superbend coil and cold mass assembly.

The production Superbends are conduction cooled, in order to place the coils as close to the ALS electron beam as possible. In the final design the diameter of the outer vacuum chamber is 54.9 mm and the Superbend poles inner diameter is 100 mm. To make the Superbend operation in the ALS as automatic, efficient, and economical as possible a 2-stage Gifford-McMahon cryocooler was used to provide the required refrigeration [12]. The 4 K heat load is minimized by the use of high temperature superconducting (HTS) leads, supplied by American Superconductor Corp., for the transition between the 50 K and the 4 K stages. Conduction-cooled copper current leads are used from room temperature to the 50 K stage. A Sumitomo Model SRDK-415 cryocooler was used after a series of cryogenic tests [16]. This cryocooler has a cooling capacity of 1.5 W at 4.2 K and 50 W at 50 K.

The connection of the cryocooler to the magnet cold mass was made by a copper link shaped in the form of an S (see Fig. 9) The function of the S-shaped link was two-fold. It was necessary to provide a good thermal connection to the cold mass while simultaneously having a weak mechanical connection to minimize the vibrations induced on the magnet poles, coils, and yokes.

To continue operation in case of cryocooler failure, the design included an 85-liter liquid helium vessel and a 35-liter liquid nitrogen vessel inside the Superbend vacuum vessel. With the reservoirs full, one can have about 24 hours of continuous running after a cryocooler failure before cryogens from external dewars need to be supplied.

The superconducting coils are wound around laminated AISI 1006 steel poles. Structural support is provided both by the poles and an outer ring of aluminum alloy 5083-H321 for structural support. In order to provide conduction cooling

to the coils, each coil is surrounded by a high-purity copper coil form that is thermally connected to the LHe vessel and cryocooler second stage. The coils are precisely mounted to the C-shaped return yoke, made out of laminated AISI 1006 steel, with bolts and locating pins.

The LHe vessel, made from 304L stainless steel, is bonded to the steel yoke with low-melting point solder to provide reasonable thermal contact. The vessel contains an internal copper heat exchanger, connected to the cryocooler second stage, to allow the helium to be continually recondensed.

The 4K cold mass (coils, yoke, and LHe vessel) is suspended with 8 straps as shown in Fig. 9. The straps are made from epoxy and unidirectional S-glass fibers for low heat load, and are designed for 2-g transportation loads in addition to the static magnet support loads. The cold mass position can be adjusted with nuts on the outside of the vacuum vessel as indicated on Fig. 8. Instrumented load washers measure the strap tension to ensure that the strap loads are adjusted correctly. With this suspension, the center of motion of the center of mass is small upon cooldown.

Tubes attached to the steel yoke allow rapid cooling with liquid nitrogen to 100 K and liquid helium to operating temperature. A warmup heater supplies 2.8 kW to the steel yoke to allow rapid warmup of the cold mass. The heater leads can be internally disconnected with a linear motion feedthrough when not in use to minimize heat loads into the 4K cold mass.

The vacuum vessel is mounted to the ALS ring girder after being positioned over the ALS storage ring vacuum chamber. Clearance allows for magnet alignment with a 6-strut suspension system.

The cryocooler cold head must be replaced every 10,000 hours with one that has been factory-reconditioned, so it was positioned to allow rapid change-out. Therefore the cold head as well as the items that were considered to require servicing and possible replacement, such as cryocooler, current leads, and quench protection diodes are readily accessible by warming the magnet to room temperature and removing the access port. In addition to the electrical heaters for rapid warmup, the cold mass is equipped with tubes for rapid cooldown. The Superbends require about 30 hours to warm from operating temperature to 300 K, 4 hours to change cryocoolers, and about 30 hours to pump down and cool from 300 K to operating temperature.

3.2.2 Quench Protection, Instrumentation, and Power Supply

The Superbend is equipped with a set of cold diodes to provide a passive means of rapidly discharging the coils in case of a quench and protection in case of a current lead failure. Fig. 10 shows the power and instrumentation schematic.

In addition, the Superbend has eight Cernox temperature sensors from LakeShore Cryotronics. Each sensor is packaged in the CU configuration and calibrated in the range 1.4 to 300 K. These sensors measure the temperature of both cryocooler stages, the warm end of both HTS leads, the copper coil forms of both coils, and the center yoke plate above and below the beam aperture gap.

Quench detection instrumentation (not shown) monitors the voltage across each of the coils and HTS leads, and the total voltage across the two magnet coils using high quality op-amps. These signals are lowpass filtered and applied to a bank of threshold detectors that send a fault signal to the power supply

if their threshold is exceeded. The fault status is latched and displayed on the front panel and made available to the accelerator control system.

The power supply was constructed by Dynapower to meet the requirements of Table 1 [13]. The power supply input is three phase 208V AC, rectified by Silicon Controlled Rectifiers (SCR) on the secondary side of the transformer. The 6-pole rectified DC voltage is filtered with a passive component network. The output current is sensed with a high quality Zero Flux Current Transformer (ZFTC), which is used as a feedback element to control the phase angle of the SCRs and consequently the output current. The power supply has an output of 350 A, ± 15 V (quadrants 1 and 4) to provide for charging and discharging the Superbend.

The current-dependent inductance of the Superbend, that ranges from 12 - 3 H, is compensated in the electronic circuitry of the feedback loop. The resistor and capacitor components in the compensation network are chosen to minimize the overshoot in the output current after the current ramp rate is changed, while maintaining the stability performance of the power supply.

The power supply is equipped with two types of external fault interlocks. The first results in a discharge with a time constant of ≈ 100 s, which will not quench the Superbend. The second results in a faster discharge with a time constant of ≈ 20 s to protect the HTS leads.

3.2.3 External Cryogenics System

In the event of cryocooler failure, the system is operated using cryogenic fluids provided by external transfer from LN_2 and LHe dewars located outside the

ALS storage ring to vessels inside the cryostat. When operating in this mode, the internal vessels are fitted with relief valves opening when the internal pressure is 0.035 bar higher than atmospheric. Liquid nitrogen provides cooling for the warm end of the HTS current leads. In addition it provides thermal shielding for the superconducting coils and the cold iron yoke from heat conducted through the leads and cryocooler. Liquid helium cools the superconducting coils and 1.5 Ton iron yoke by means of copper conduction paths.

3.2.4 Fiducialization and Alignment

The pole tips, return yoke and vacuum vessel have features to enable the ALS Survey team to position the cold mass at the correct position in the cryostat using optical tooling. Final positioning is done with the 6-strut suspension, based on magnetic measurements of the magnetic center and magnet roll.

3.3 System Performance

Various subsystems of the cryogenic system were tested individually and later the full magnet systems were tested to ensure the feasibility of the system. It was necessary to verify that under normal operation the Superbends could be cooled without external cryogenics and that the various components were robust. Early on in the project a test setup was constructed to test the feasibility of conduction cooling and in particular the cryocooler, and the HTS leads [16]. The results were successful providing confidence in the cryogenic scheme.

After construction of each of the Superbend magnets, extensive cryogenic tests

of the Superbends revealed problems on 2 of the 4 magnets. Again, because the tests were carried out early enough, the problems could be fixed without impact on the overall time schedule.

Table 4 presents the range of measured Superbend temperatures for the case of refrigeration provided by the cryocooler with the magnets operating at 300 A.

The temperatures in Table 4 lie close to the expected values and demonstrate that the cryogenic design goals are met. No cryogenic fluids are consumed as long as the cryocooler is operational. The variation in temperature is dependent upon the performance of the particular cryocooler cold head installed.

An important operational parameter is the rate at which the magnets can be ramped from the injection current of 217 A, corresponding to 1.5 GeV beam energy, to 298 A, corresponding to the 1.9 GeV nominal operating point. Tests demonstrated that the magnets can be reliably ramped at 1 A/s when operating with the cryocooler. The limitation is due to eddy current heating in the conductor. Prior to installation the Superbends were cycled a minimum of 1000 times between the above current limits at 0.8 A/s to establish confidence in reliable operation. In addition, one of the Superbends was cycled 5000 times to simulate more than four years of operation.

3.3.1 External Cryogenics System Tests

The backup cryogenic system was tested to ensure that the Superbends could transition smoothly to external cryogenic operation in the event of a cryocooler failure. Prior to the Superbend installation one of the Superbends was tested

and it was found that if the LN_2 level is maintained above 30% the temperature of the warm end of the HTS lead remains at 84 K or less as, which is within the specification of the HTS lead. The 35 l LN_2 vessel must be refilled about every 14 hours to maintain this level. For that Superbend the temperature of the coils is maintained at 4.8 K or less when the helium level is greater than 50%. This requires that we transfer liquid helium about every eight hours.

3.3.2 Vibration Testing

Cold mass motion induced by the cryocooler was measured with Model 731A seismic accelerometers from Wilcoxon Research. The measurements revealed that the 4 K thermal connection was the main pathway for induced vibrations. These measurements lead to a design change. The cold-head of the cryocooler induced significant (about one μm amplitude) vibrations of the cold mass. This was found in measurements with high precision accelerometers. A modification of the thermal link between the cold-head and the magnet solved the problem.

After the design change was implemented the vibrations were reduced well below the required values summarized in Table I. The 50 K thermal connection and the mounting of the cold head to the Superbend vacuum vessel bellows played no significant role in cold mass motion. Fig. 11 shows a comparison of the cold mass vibration with the cryocooler on and off, after the thermal connection between the second stage of the cryo cooler and the cold mass had been optimized in order to minimize the cold mass vibration. Except for some small effects at frequencies above 60 Hz, there is virtually no difference in the magnitude of the vibrations with cryo cooler on and off.

In addition, other measurements were carried out in the ALS tunnel which ver-

ified before the actual Superbend installation that transmission of cryocooler vibrations to neighboring magnets is not a problem. Those measurements were conducted by mounting a cold head with a temporary fixture to one of the normal bending magnets to be replaced with the Superbends. With the cryo cooler active, the vibrations transmitted to all neighbouring magnets were very similar to the situation with the Superbends installed. For these measurements again accelerometers were used as well as directly measuring the impact of the vibrations of the quadrupoles and dipoles on the beam using beam position monitors. We saw very small additional vibration of neighboring magnets below our tolerance levels. The orbit measurements showed no additional orbit jitter.

3.3.3 Power Supply Tests

To preserve the good orbit and beam energy stability of the ALS, the power supplies of the Superbends are especially stable (5 ppm) and they stay always connected to the magnet. At the same time measurements confirmed that the existing power supply of the main bending magnet chain fullfills the same stability requirement. The measurements actually revealed minor problems with some of the power supplies, but since they were carried out early, corrections to the power supply compensation loops could be made in time to achieve design performance by the start of commissioning with beam.

3.4 Magnetic Measurements

Multipole measurements are made to insure that field quality tolerances are met and to locate the magnetic axis. Fig. 12 below, shows a picture of the

first Superbend installed around an alignment fixture on the test stand. Both the cryostat and the alignment fixture are mounted with six struts allowing for adjustment in all degrees of freedom.

The alignment fixture serves several important functions in the testing process [10]. A cylindrical bore coincident with the electron beam axis is drilled through the alignment fixture. The bore is used to position measurement coils and probes. As explained below, multipole measurements are used to position the magnet and cryostat so that the magnetic axis and measurement, or alignment fixture bore, axis coincide. Fiducials on the alignment fixture are used to relate this axis to fiducials on the cryostat, which are then used as survey marks for installation at its correct position in the ALS lattice. The alignment fixture is machined with the same profile as the Superbend cutout in the storage ring vacuum chamber, thus insuring correct fit during installation. Magnetic measurements were conducted in the range between 200 A and 300 A.

3.4.1 Sextupole and Higher Order Multipoles

Multipoles were measured with a 1 m long integral search coil [10]. The measured value for the normalized sextupole varied between 3.20×10^{-3} and 3.26×10^{-3} for the four magnets, easily meeting the specifications (see Table 1. The sextupole value agrees very well with the design value of 3.23×10^{-3}, determined from three-dimensional finite element models using the Tosca code. All higher order multipoles were less than 1×10^{-4} which also meet the specifications in Table 1.

3.4.2 Radial and Vertical Position

The transverse and vertical magnetic center is defined as the center of the sextupole, the dominant multipole component. In the absence of other asymmetries giving rise to a quadrupole, this is the location where the quadrupole component is zero.

The first step in the magnetic measurement process for each of the four Superbend magnets was to determine the radial and vertical positions. Setting the magnet current at 250 A, roughly in the middle of the normal operating range, measured values of the quadrupole and sextupole were used to position the magnet assemblies in order to cancel the normal and skew quadrupole components. Table 5 shows the remaining error for all four magnets after the final adjustment. They meet the specifications in Table 1.

Then measurements showed that the normal quadrupole component shifted systematically with current. This is caused by the opening and closing of the magnet yoke, thus changing pole angles, due to magnetic forces. However, all measured values are well within the specified tolerance.

3.4.3 Magnet Roll

The magnet roll tolerance of 0.25 mrad (compare Tab. 1) is based on the allowable vertical orbit distortion during routine operation of the storage ring. During the design phase, the difficulty of measuring and adjusting the roll to this precision was recognized. Additional electron beam dynamics studies showed that as much as 2 mrad of roll could be tolerated without compromising the ability to inject and store electron beam without local orbit correction. To

have a fallback solution in case the magnetic measurements would not achieve the tighter precision of 0.25 mrad, a set of trim coils was designed and installed on all Superbends to produce a skew dipole field, allowing for roll adjustment of several mrad. This way the trim coils could have been used for fine tuning based on beam orbit measurements.

To measure the angular field orientation — and therefore the magnet roll — an apparatus incorporating a Hall probe and a precision tilt sensor, with 5 μrad resolution was used. The Hall probe and tilt sensor holder is attached via a connection rod to a rotating stage, allowing measurement scans of field vs. angle. The rod is inserted into the same alignment fixture bore used to locate the integral search coil, thus insuring roll measurements are done about the magnetic axis. The connection is designed so that the Hall probe and tilt sensor can be inserted from either end of the alignment fixture.

This setup allowed for the detection of the angular orientation of field zero as well as field peak. The field zero detection method proved to be unrepeatable due to a strong planar field in the Hall probe at the zero field orientation [9]. The field peak detection method, however, proved to be very repeatable.

Effective roll is defined as a weighted average of the roll values measured at the different longitudinal locations, where the weighting factors are based upon the axial field distribution. The uncorrected, effective roll for the four Superbend magnets at the two operating currents, 212 A and 300 A, corresponding to roughly 1.5 and 1.9 GeV, was less than 1.1 mrad for all Superbends. The final error in the determination of the magnet roll turned out to be smaller than the original tolerance of 0.25 mrad. Therefore the inclusion of the trim coils ultimately was not necessary. However, it did ensure that the project stayed

within the original time schedule, since it provided a fall back solution while the magnetic measurement methods were refined to ultimately achieve this accuracy.

3.4.4 Longitudinal Field Profile

Axial field profiles were used to measure the longitudinal magnetic center and field integrals. They were measured with a Hall probe attached to the end of the integral coil housing. A linear stage incorporated into the integral coil setup allows field scanning along the same axis as is used for the multipole and roll measurements. Fig. 13 shows a plot of axial field profiles at 212 A and 300 A for one of the magnets which corresponds to roughly 1.5 and 1.9 GeV.

The axial magnetic center is defined as the location, z_0, for which the downstream field integral equals the upstream field integral.

$$\int_{-\infty}^{z_0} B_y dz = \int_{z_0}^{\infty} B_y dz \tag{1}$$

For a symmetric distribution, this also corresponds to the peak field location. The magnetic center must be determined and the magnet placed into the ring accordingly to within 1 mm in order to meet the tolerance for horizontal orbit distortion. The measured difference between the peak field location and the half-integral point is less than 0.1 mm for all four magnets.

4 Precommissioning

In order to ensure that the transition to Superbend operation was transparent, the Superbend team adopted the strategy of precomissioning as many subsys-

tems (with and without beam) as possible prior to the actual installation of the Superbends. Much of the work has already been described earlier.

To minimize the impact on users, the Superbend installation was split into two medium length (6 week) shutdowns. In the first shutdown (which occurred in March 2000) all major components of the project, excluding the actual Superbend magnets were installed [14]. In the second shutdown (which began in August 2001) the Superbends were installed and commissioned [15].

As discussed in the previous section, the Superbend systems were extensively modeled and tested. The team performed thorough cryogenic testing, magnet measurements, vibration testing, powersupply and controls testing. The results of these tests showed that the system was very reliable. Now we discuss the tests of systems other then the Superbend magnets.

As mentioned before, most non-Superbend items were installed more than one year before the actual commissioning. This included the new quadrupoles around the three Superbend locations (QDA magnets in Fig. 3) which make up for the loss of the horizontally defocusing quadrupole field which the replaced normal conducting bending magnets provided before. Also installed were new power supplies for the other quadrupoles in the arcs which would house the Superbends, to provide the possibility to minimize the periodicity breaking. Both of those early upgrades also enabled early studies of the effect of the Superbends on the nonlinear dynamics, by allowing the simulation of the breaking of the lattice periodicity due to the Superbends. Furthermore the control system was upgraded, to allow better synchronization of all magnets during the energy ramp between 1.5 and 1.9 GeV, as well as better stability and noise performance of the D/A converters and additional diagnostic capa-

bilities. The complete storage ring was aligned, which provided the possibility of skipping a complete alignment during the actual installation shutdown of the Superbends, minimizing the risk and potential complications for the Superbend commissioning. The main storage ring vacuum chambers at the future Superbend locations were machined in situ to allow the cryostats to fit (see Fig. 14). The ALS vacuum chambers are precision machined aluminum vessels with machined pockets for all magnet poles to minimize the distances of the magnet poles to the beam. Since the Superbend pole and cryostat shape is very different from the gradient bend magnet it replaces, significant remachining was necessary.

4.1 Beam Dynamics Tests

As mentioned earlier one of the main concerns of the Superbend project was related to their possible impact on the dynamic aperture and dynamic momentum aperture and therefore on injection efficiency and lifetime. In particular there was concern about the reduction in the lattice periodicity. In general having a high degree of periodicity helps to improve the beam dynamics. In a ring with P fold periodicity structural betatron resonances may only occur when the following condition is satisfied:

$$N_x \frac{\nu_x}{P} + N_y \frac{\nu_y}{P} = M \tag{2}$$

where ν_x and ν_y are the horizontal and vertical betatron tunes for the full ring and N_x and N_y and M are integers. Lower periodicity can lead to stronger resonance excitation, potentially reducing the dynamic aperture and dynamic momentum aperture. An illustration of the benefits of high periodicity is shown

in Fig. 15 where all allowed resonances (those satisfying Eqn. 2) are plotted up to 5th order ($|N_x| + |N_y| \leq 5$) for the case of 12 and 3 fold periodicity. One can see that there are many more low order resonances that might be excited in the case of 3-fold periodicity.

There are several reasons that the Superbends perturb the lattice periodicity. The Superbends had to be built as plain dipole magnets. Since they replace gradient bending magnets with a significant horizontally defocusing quadrupole field, the original 12-fold periodicity of the lattice inevitably was broken. In addition, the Superbends have a very significant systematic sextupole field. This of course adds to the breaking of the 12-fold lattice periodicity, resulting in an effective 3-fold periodicity.

For the ALS, which operates in a fully Touschek lifetime dominated regime, it turned out that the main concern was the dynamic momentum aperture, which strongly affects the Touschek lifetime. The Superbends did change the dynamics significantly. But the goal was to ensure that the change in dynamics did not have a large effect on injection efficiency or lifetime.

For all these reasons extensive studies of the non-linear dynamics were carried out both in simulation and experiment. The technique of frequency map analysis was developed and heavily used [21,22,26]. The effects of the Superbends on the non-linear dynamics were experimentally studied in the real machine before the actual Superbend installation by using the new quadrupoles around the Superbends to simulate the periodicity breaking.

4.1.1 Theoretical Studies

The tracking studies led to an early improvement in the lattice, when it was found, that by just keeping the overall horizontal phase advance in all 12 arcs the same, the dynamic aperture with small machine errors was virtually identical to the original 12-fold periodic machine. In this lattice, the local phase advance between the sextupoles in the three Superbend arcs is still different from the other 9 sectors, but the effect of that was negligible. Fig. 16 shows the dynamic aperture and on-energy frequency map displayed in amplitude as well as tune space with the lattice before and Fig. 17 the one after Superbends. The frequency maps were calculated including machine errors corresponding to a beta beating of about 1% and an emittance ratio of about 1% as well as a vertical aperture of ± 4 mm in representing the narrow gap insertion device chambers in the straights. The diffusion rate of the particles is indicated by the color (the color scale is logarithmic) [22]. Initial conditions of particles with high diffusion are plotted in red and those with low diffusion are plotted in blue.

One can see that in both cases the dynamics is well behaved horizontally up to 12 mm which is more than sufficient for a $\leq$10 mm injection offset of the ALS. Above a horizontal amplitude of 12 mm, both frequency maps show fairly large areas of high diffusion indicating the possibility of particle loss in the vertical plane. Therefore the horizontal dynamic aperture relevant for injection in both cases is about equal. In the vertical plane, the dynamic aperture at larger horizontal amplitudes is smaller in the lattice with Superbends and distributed dispersion, however, this does not have any significant performance impact.

In frequency space, the two maps look significantly different. The detuning with amplitude is bigger in the case with Superbends and resonance excitation differs in strength. This difference is mostly caused by the non-zero dispersion lattice used with the Superbends. The symmetry breaking due to the Superbends in fact has a smaller impact after optimizing the lattice. The main limitation in the pre Superbend lattice occurs at (ν_x=14.2 and ν_y=8.1) where an unallowed third order (ν_x-2ν_y=-2) and an unallowed fifth order (5ν_x=71) resonance intersect. This intersection in frequency space corresponds to the broad diffusive region above 12 mm horizontal amplitude in configuration space. In the Superbend lattice due to the change in tuneshift with amplitude the (5ν_x=71) resonance is crossed at a different point and at lower amplitudes. The main limitation is the diffusive region around (ν_x=14.17 and ν_y=8.1) which corresponds to the diffusive region beyond 12 mm horizontal amplitude in configuration space. Overall these studies predicted that even though the details of the transverse dynamics change significantly with Superbends the impact on injection efficiency would be minimal.

4.1.2 Experimental Studies

Before installing the Superbends, the ALS had always operated with a lattice with zero horizontal dispersion in the straights. It would have always been possible but not reasonable to operate with lower horizontal emittance since the Touschek lifetimes would have been too small (because the Touschek lifetime is roughly proportional to the bunch volume). With Superbends it was planned to use a distributed dispersion lattice to minimize the horizontal emittance increase. This lattice was tested extensively before the Superbend installation. The tests of its properties in terms of nonlinear dynamics are de-

scribed in the following paragraphs and showed that it was feasible to use this lattice. In addition, it was verified that without Superbends the distributed dispersion lattice provided the predicted reduction in horizontal emittance (of close to a factor of two).

The predictions of the on-energy and off-energy dynamics models for the performance with Superbends described above were experimentally tested prior to the actual installation of the Superbends. Using the quadrupole magnets next to the future Superbend locations that were installed in the first shutdown, the periodicity of the ring was perturbed to the degree of the Superbend lattice and off energy frequency maps and lifetimes were measured.

The results of the first momentum aperture measurement with the simulated periodicity breaking showed actually a large reduction in momentum aperture. The reason was that with the lower 3-fold periodicity, a previously not excited resonance ($3\nu_x + \nu_y = 17 \times 3$) suddenly became allowed by periodicity and was therefore strongly excited. Because of this resonance, the momentum aperture became very sensitive to the exact values of the chromaticities. By looking at the frequency analysis of the data, the reason for the drop in momentum aperture became immediately obvious. It was then predicted that by slightly reoptimizing the sextupole settings, the expected momentum aperture (which is virtually identical to the one without Superbends) could be recovered, which was verified experimentally. After reoptimization, the dynamic momentum aperture for the distributed dispersion lattice with the simulated symmetry breaking due to 3 Superbends remained close to the RF acceptance at 2.5% (compare left side of Fig. 18). These tests agreed well with our model predictions.

During those studies it was also found, that for the lattice with equal total horizontal phase advance over all arcs, it would even be possible to place just one or two asymmetric Superbends, yielding a lattice periodicity of one, with acceptable dynamic aperture and dynamic momentum aperture for a zero dispersion lattice (compare right side of Fig. 18). Those studies were important to provide fall back scenarios, in case not all Superbend magnets would have been ready by the time of the planned installation shutdown. Since the user demand for the new Superbend beamlines was extremely high, it would have been possible to go ahead with a partial installation. In the end, the studies were helpful in keeping the installation shutdown on schedule, since it turned out that the spare magnet was finished late enough, that without the availability of this fall back scenario, the installation could have been delayed.

4.2 Installation and Commissioning

The installation and commissioning of the Superbends occurred in a 6 week period that began on August 20, 2001 and ended on October 3, 2001. A picture of the first Superbend being installed can be seen in Fig. 19. The installation period lasted for 11 days. During that time 3 normal magnets were removed, 3 Superbends installed, and a portion of the injection line disassembled and reinstalled. In addition the new controls, power supplies, diagnostics, and external cryogenics were installed and tested.

After the installation was finished on August 30, 2001, the commissioning [15] was very successful right from the start: Fig. 20 shows the current history of the first commissioning day. First beam was stored just after midnight, 5 minutes after trying to inject. For the initial commissioning, a zero dispersion lattice

was used, which was easier in terms of the nonlinear dynamics. The alignment and field calibration of all new elements was good enough and the lattice set well enough that only some steering of the transfer channel from the booster synchrotron was necessary. Within one hour, 100 mA were stored (limited by vacuum pressure due to outgassing of new Superbend photon stops). On the same afternoon, beam was ramped successfully from the injection energy of 1.5 GeV to the normal operation energy of 1.9 GeV showing that all field measurements were accurate and control system and power supplies worked well.

The commissioning continued at a quick pace. After correcting the lattice periodicity using the results of an orbit response matrix analysis, the nonlinear dynamics properties of the lattice were measured. The dynamic aperture and momentum aperture were about the same as before the Superbends. All details (because of the change in lattice periodicity, many details of the measurements changed) agreed extremely well with the predictions of simulations. More details of those measurements are given in the next subsection.

The orbit stability and orbit jitter were measured (see Fig. 21). They were virtually the same as before the installation of the Superbends (as expected after the design change due to the vibration measurements and the measurements of all and optimization of some power supplies). Horizontal emittance (10.5 nm) of the zero-dispersion lattice and coupling (emittance ratio below 1%) were measured and agreed well with the predictions.

4.2.1 Experiments concerning Transverse Nonlinear Dynamics

As mentioned earlier, injection efficiency and lifetime were among the main concerns associated with the Superbend upgrade. Therefore extensive studies, both in simulations and using experiments with simulated periodicity breaking due to the Superbends were carried out in advance (compare earlier sections). During the commissioning all properties related to the nonlinear dynamics were measured again in great detail. The measurements were first carried out for the Superbend lattice with zero disperion in the straights and later with 6 cm of dispersion in the straights.

The nonzero dispersion Superbend lattice had significantly lower horizontal emittance than the zero dispersion lattice yet it still had a slightly higher (20%) horizontal emittance than the pre Superbend lattice. The reduction in brightness coming from this larger horizontal emittance was compensated by reducing the vertical emittance. The resulting lifetime compared with the pre Superbend lattice remained unchanged. Overall, the new lattice provides about the same brightness to users of soft x-ray undulators and normal bend magnets as before Superbends.

The non zero dispersion lattice was then characterized. Because it reduces the dispersion in the arcs (i.e. at the location of the sextupoles), it requires significantly higher sextupole strengths, thereby increasing nonlinearities and the strength of resonances. The easiest way to quantify the impact on the lifetime is to measure the momentum aperture using a scan of the RF-acceptance. The Touschek lifetime τ_{tou} is proportional to:

$$\tau_{\mathrm{tou}} \propto E^3 \frac{V_{\mathrm{bunch}} \sigma_x'}{I_{\mathrm{bunch}}} \varepsilon^2 f\left(\varepsilon, \sigma_x', E\right), \tag{3}$$

where E is the beam energy, V_{bunch} is the bunch volume, I_{bunch} is the bunch current, σ'_x is the horizontal beam divergence, ε is the momentum aperture and f is a complicated integral function with relatively weak dependence on its arguments. The vertical emittance was adjusted in both the zero and non zero Superbend lattices so that the total bunch volume (see Eqn. 3) was the same as the corresponding lattice before Superbends. As one can see, the Touschek lifetime depends rather strongly on the momentum aperture and of course the beam energy, which is the reason why it is such a dominant concern at low energy third generation light sources like the ALS.

So if the beam lifetime is Touschek dominated one expects a (slightly more than) quadratic dependence on the RF-acceptance, as long as it is the smallest aperture in momentum space. The point where the lifetime deviates from the quadratic behaviour is where other apertures become important. For the ALS the first one is the dynamic momentum aperture in the arc. As one can see in Fig. 22, the momentum aperture for the distributed dispersion lattice is indeed slightly smaller than for the zero dispersion lattice. But there is little difference between both cases with and without Superbends. All values agree very well with predictions based on tracking studies. At 1.9 GeV, the available RF-voltage at full beam current corresponds to an RF-acceptance of about 2.5%. This is very close to the measured dynamic momentum aperture for the distributed dispersion case. Therefore the reduction in lifetime at 1.9 GeV due to the dynamic momentum aperture is small (as long as the beta-beating is corrected to less than 1% rms).

Measuring the off-energy dynamic aperture (compare Fig. 23) provides results for the momentum aperture, which are very consistent with the direct quantitative measurement using the rf-amplitude scan. By using frequency

analysis on the measurement results, one can also get detailed information about which resonances or diffusive areas in tune space are dominating the momentum aperture (compare right side of Fig. 23). Again, all details of those results are in very good agreement with simulations and predictions.

Overall, the Superbend upgrade proved how powerful the simulation and experimental techniques based on frequency map analysis are. Even though the periodicity of the lattice was reduced from 12 to 3, many details of the dynamics changed and the lattice is now pushed very close to its limits, the performance was predicted very accurately in advance and negative effects on the performance could be avoided.

5 Operational Experience

Immediately following the installation of Superbends, the lifetime was the same as before, fast orbit stability was the same, slow orbit stability was better, injection and ramping times were comparable and there was a small change in the beam sizes (see Table 6) and no noticable change in brightness for normal bend magnet and undulator users [15]. As time has passed, the performance of the machine has continued to improve well beyond pre Superbend operation. There have been developments in fast and slow orbit feedback systems significantly improving the orbit stability particularly in the bend magnet beamlines. There have been developments in vertical beamsize control allowing the machine to operate with smaller vertical apertures and thus higher performance insertion devices.

5.1 Overall Reliability

Since the installation of the Superbends there have been more than two and a half years of nearly continous operation of the ALS. During this time the Superbends have been extremely reliable. Superbend system failures have accounted for a small fraction of the total downtime of the ALS. In fact the largest portion of the downtime that was related to operating with Superbends was that the ALS initially experienced in increase in the failure rate of conventional waterflow meters on photon stops — many of which were located downstream of the Superbends and were failing due to the increased radiation exposure. The problem was solved quickly by adding lead shielding around every water flow sensor.

5.2 Cryo System Performance

The cryosystem in particular has proven to be very reliable. The operating temperatures, magnet currents and cryo system pressures for one week of two-bunch operation are shown in Fig. 24. Because of the high electron density the beam lifetime in two-bunch operation is much shorter than during the more common multibunch operation of the ALS. Therefore injections occur every 2 hours compared to every 8 hours during multibunch operation. The eddy current induced heat input to the cryo system is highest in this operation mode. So the figure shows the performance in a worst case scenario.

There has only been one failure of the cryosystems so far. This occurred in March 2003 two weeks prior to a four week scheduled shutdown of the ALS (compare Fig. 25). On one of the Superbends the cryocooler stopped func-

tioning. This Superbend ran with external cryogens for 2 weeks following that failure. The failure resulted in a total downtime of 6 hours. Part of that downtime was due to attempt to restart the cryocooler and part was due to modifications in some controls software to reduce the ramping rate. The operation of Superbends with the cryogens went smoothly with no further downtime. This experience demonstrated the feasibility of operation with cryogens and convinced us that in the case of future failures one should be able to transition between cryocooler and cryogenic operation without any downtime.

5.3 Impact of Superbends on the ALS

There has been a large demand for Superbend beamlines. At the time of this paper, 7 of the 12 beamlines are in operation — 5 for protein crystallography, 1 for tomography, and 1 for high pressure diffraction. This still leaves 5 beamlines which have yet to be committed. Of the 5 protein crystallography beamlines, 3 have been in operation for about two years and have performed extremely well and have contributed to the solution of many protein structures[5]. With the Superbend upgrade the ALS has greatly extended its capacity and capability in the hard x-ray regime. Already in the ALS's second year of operation with Superbends, the number of annual Superbend beamline users has exceeded 300 — approximately 20% of the total number of users at the ALS. Most of those users are on the three initial Superbend beamlines. The number will continue to grow as more of the beamlines are completed and commissioned.

6 Summary

Looking back one can say that the Superbend project met all, and in many cases exceeded, the project goals. The project was completed on time. All performance goals (brightness, lifetime, fill times, and stability) have been achieved. The transition to Superbend operation was transparent with no significant impact on the non-Superbend users. Moreover, there was no significant Superbend related reduction in reliability as compared with pre Superbend operation. With the successful completion of the Superbend project the ALS has transformed itself, greatly increasing its capability and capacity to deliver bright hard x-ray beams.

7 Acknowledgements

There are many who the authors wish to acknowledge. Alan Jackson and Verner Joho for initially proposing the idea of the Superbends. Members of the team which produced and tested the first successful prototype of the coils and core — particularly Alan Lietzke, Shlomo Caspi, and Ronald Scanlan. The authors wish to thank Shlomo Caspi and Etienne Forest from KEK for helping to simulate the effect of the 3D field on the beam dynamics. The authors with to thank Prof. Ying Wu from Duke University for helping with the vibration measurements. The authors wish to thank Kem Robinson for his productive reviews of the project. The authors wish to thank the staff of the ALS. Finally the authors wish to thank the generous support of the management of Lawrence Berkeley National Laboratory and the Advanced Light Source Division, Accelerator Fusion Research Division and the Engineering Division. In

particular we wish to thank Charles Shank, Brian Kinkaid, Daniel Chemla, William Barletta, and Benedict Feinberg.

References

[1] B. G. Levi, "Gamble Pays Off at the Advanced Light Source", Physics Today (2002), January; 55, pp. 17

[2] D. Robin, A. Robinson, L. Tamura, "Superbends expand the scope of Berkeley's ALS", CERN Courier, (2002), March; Vol. 42, No. 2, pp. 28-31

[3] L. Tamura and A. Robinson, "Superbends Era Begins Swiftly at the ALS", Synchrotron Radiation News, (2002); Vol 15, No. 1, pp. 30-34

[4] D. Robin et.al. "Successful Completion of the Superbend Project", Proceedings of the 2002 European Particle Accelerator Conference, (2002) pp. 215-217

[5] A. MacDowell, et al,"Suite of Three Protein Crystallography Beamlines with Single Superconducting Bend Magnet as the Source," Submitted to Journal of Synchtrotron Radiation, (2004)

[6] R. Service, "Upgrade Brings Hope to Berkeley's Advanced Light Source", Science (1999) August 27; 285, pp. 1344

[7] R. Service, "Wiggling and Undulating Out of an X-ray Shortage", Science (1999) August 27; 285, pp. 1342-1346

[8] C. E. Taylor and S. Caspi, "A 6.3 T Bend Magnet for the Advanced Light Source", IEEE Trans. Magnetics 32, No. 4, (1996), pp. 2175-2178

[9] C. E. Taylor, et al., "Test of a High-Field Magnet for the ALS", Transactions on Applied Superconductivity 9, No. 2, (1999), pp. 479-482

[10] "Superbend Magnet System Conceptual Design Report", Lawrence Berkeley National Laboratory Publication, PUB-5457, Apr. (2000)

[11] E. Hoyer and J. Zbasnick, "Superbend Magnet Specification", Lawrence Berkeley National Lboratory Specification M909, Nov. 1999

[12] M. A. Green, et al., "Refrigeration options for the ALS Superbend dipole magnets", to be published in proceedings of the 1999 CEC, Montreal, Quebec, Canada, July 1999.

[13] G. J. DeVries, "Superbend magnet power supply specification," Lawrence Berkeley National Laboratory Specification LSE-128.

[14] D. Robin, et al., "Superbend Project at the Advanced Light Source", Proceedings of the 2001 IEEE Particle Accelerator Conference, Chicago, 2632 - 2634 (2001)

[15] C. Steier, et al., "Commissioning of the Advanced Light Source with Superbends", European Particle Accelerator Conference, 754 -756 (2002)

[16] J. Zbasnik, et al., "Test of a GM cryocooler and high Tc leads for use on the ALS Superbend magnets", Published in the proceedings of the (1999) CEC, Montreal, July 1999

[17] J. Zbasnik, et al., "ALS Superbend Magnet System", IEEE Trans. on Applied Superconductivity, Vol. 11, No. 1, March, (2001), pp. 2531-2534

[18] S. Marks, et al., "ALS Superbend Magnet Performance", Published in the proceedings of the 17th International Conference on Magnetic Technology, Geneva, (2001)

[19] S. Caspi, M. Helm, and L. J. Laslett, "The use of harmonics in 3-D Magnetic Fields", IEEE Trans. Magn. Vol. 30, No. 4, (1996)

[20] H. Nishimura and D. Robin, "Impact of Superbends at the ALS", Proceedings of the 1999 IEEE Particle Accelerator Conference, New York, (2001) pp. 203 - 205

[21] D. Robin, C. Steier, J. Laskar, L. Nadolski, "Global Dynamics of the Advanced Light Source Revealed through Experimental Frequency Map Analysis", Phys. Rev. Lett. 85, 3, p. 558 (2000).

[22] C. Steier et al., "Measuring and Optimizing the Momentum Aperture in a Particle Storage Ring", Phys. Rev. E 65, 056506 (2002)

[23] See for example G. Rudenko et. al., Science **298**,2353 (2002) and E. Yu. Science **300**, 976 (2003)

[24] 1-2 GeV Synchrotron Radiation Source Conceptual Design Report, LBNL publication *PUB-5172 Rev.* (1986).

[25] D. Robin, J. Safranek, W. Decking, "Realizing the benfits of restored periodicity in the advanced light source", Physical Review Special Topics - Accelerators and Beams, Volume 2, 044001 (1999)

[26] C. Steier et al., "Lattice Model Calibration and Frequency Map Measurements at the ALS", Proceedings of EPAC 2000, p. 1077, Vienna, Austria.

Table 1

SUPERBEND MAGNETIC REQUIREMENTS

Quantity	**Value**
Peak Field	5.69 T
Field Integral (1.9 GeV)	1.105 T-m
Sextupole (systematic)	$\leq 60 \times 10^{-4}$ relative to the dipole at 1 cm
Higher Order	$\leq 2 \times 10^{-4}$ relative to the dipole at 1 cm
Sextupole (random)	$\leq 3 \times 10^{-4}$ (peak to peak) at 1 cm
Longitudinal Position	Within $\pm$ 1 mm of ideal
Radial Position	Within $\pm$ 0.5 mm of ideal
Vertical Position	Within $\pm$ 0.4 mm of ideal
Roll	$\leq 250\mu$rad
Longitudinal Vibration	$\leq 3\mu$m for frequencies > 0.01 Hz
Radial Vibration	$\leq 5\mu$m for frequencies > 0.01 Hz
Vertical Vibration	$\leq 5\mu$m for frequencies > 0.01 Hz
Rolling Motion	$\leq 2\mu$rad for frequencies > 0.01 Hz
Field Ripple	$\leq 5 \times 10^{-6}$ for frequencies > 0.01 Hz
	$\leq 1.7 \times 10^{-5}$ for frequencies ≤ 0.01 Hz

Table 2

SUPERBEND CONDUCTOR SPECIFICATION PARAMETERS

Quantity	**Value**
Type	Monolithic, NbTi/Cu
Cu:NbTi ratio	3.0
Number of filaments	330
Filament Diameter	39 microns
Twist Pitch	26 ± 2 mm
Insulation	Formvar
Dimensions (bare)	0.9 mm × 1.8 mm
Dimensions (insulated)	1.00 mm × 1.90 mm, 0.02 mm
RRR	200

Table 3

SUPERBEND MAGNET OPERATING PARAMETERS

Quantity	**Value**
Magnet type	Racetrack windings, iron poles
Pole length along beam	114 mm
Pole length transverse to beam	180 mm
Turns per layer	33
Number of layers	70
Conductor length per coil	1725 m
Operating current	298 A at 1.9 GeV
Current sharing temp	value is 5.23 K at 298A
Peak field at conductor	6.8 T
Fraction of critical current	0.5 at 4.3 K
Stored energy	150 kJ
Low-field inductance	11 H
High-field inductance	3 H
Total cold mass	1500 kg

Table 4

MEASURED TEMPERATURE RANGES AT I = 300 A FOR THE SUPER-BENDS

	Temperature Ranges in K
Stage 1	38.8 to 45.2
Stage 2	3.56 to 4.05
HTS Lead A	56.5 to 58.1
HTS Lead B	56.5 to 59.1
Upper Coil	3.98 to 4.37
Lower Coil	4.01 to 4.41
Upper Yoke	4.17 to 4.55
Lower Yoke	4.21 to 4.60

Table 5

MEASURED TRANSVERSE CENTER VALUES AFTER FINAL POSITIONING

I [A]	$\mid \Delta x \mid$	$\mid \Delta y \mid$
200	$< 250\mu$m	$< 100\mu$m
250	$< 50\mu$m	$< 100\mu$m
300	$< 350\mu$m	$< 250\mu$m

Table 6

Comparison of parameters before and after Superbends at the insertion device beamline (.0) and the bend magnet beamlines (.1, .2, .3, .4)

Parameter	**Before Superbends**	**After Superbends**
Natural emit.	5.5 rad nm	6.75 rad nm
Energy spread	0.08%	0.1%
Beamline	Hor. beam size	Hor. beam size
x.0	250 μm	310 μm
x.1	50 μm	57 μm
x.2 and x.3	100 μm	100 μm
x.4	60 μm	65 μm
Beamline	Ver. beam size	Ver. beam size
y.0	30 μm	23 μm
y.1	65 μm	54 μm
y.2 and y.3	20 μm	15 μm
y.4	60 μm	52 μm

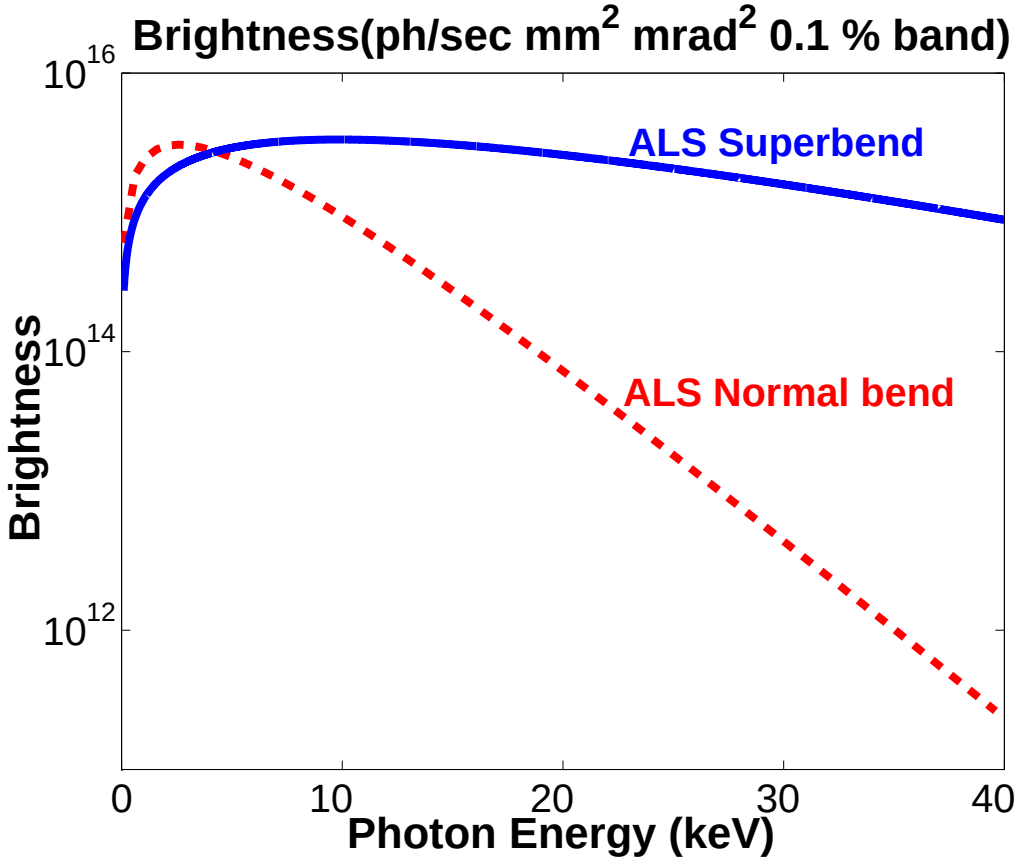

Fig. 1. Brightness of a Superbend versus the normal conducting bend

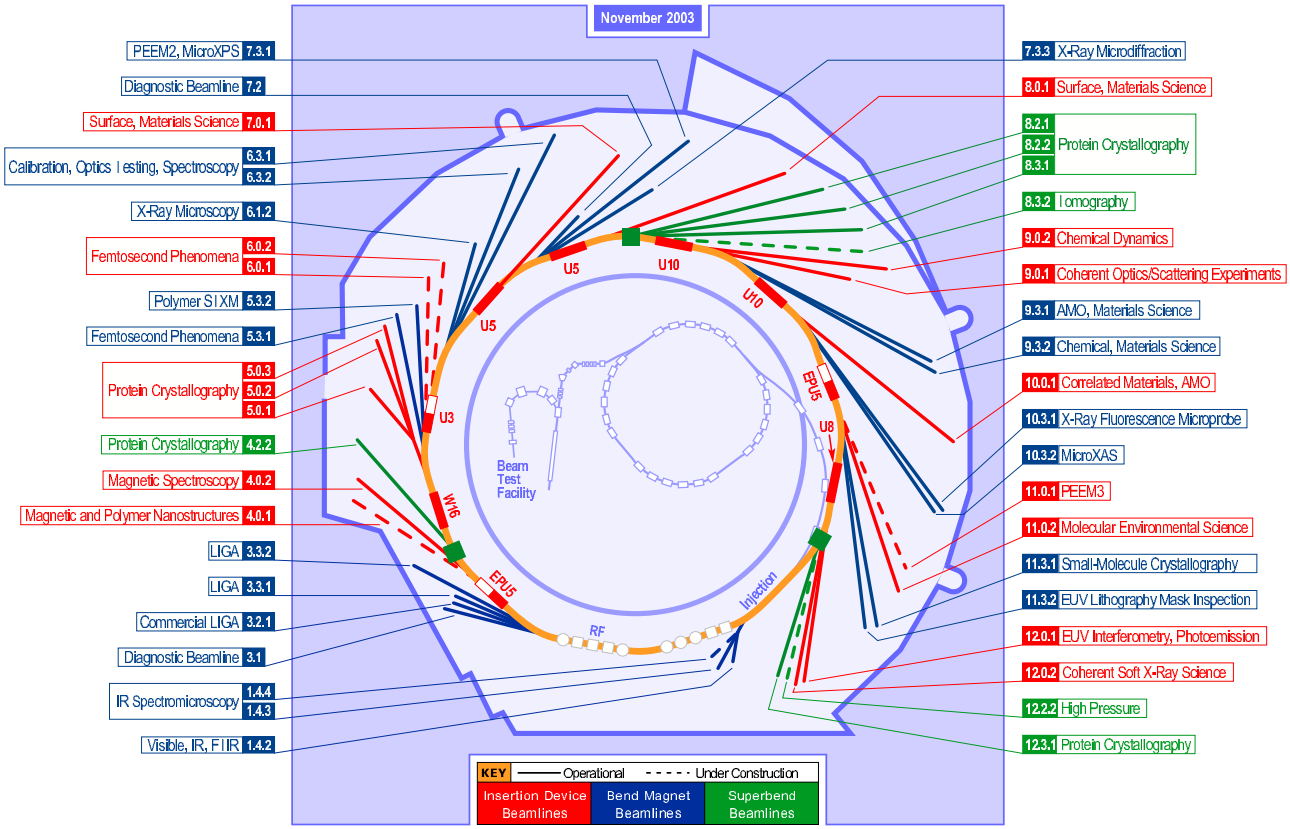

Fig. 2. Clock diagram of the ALS

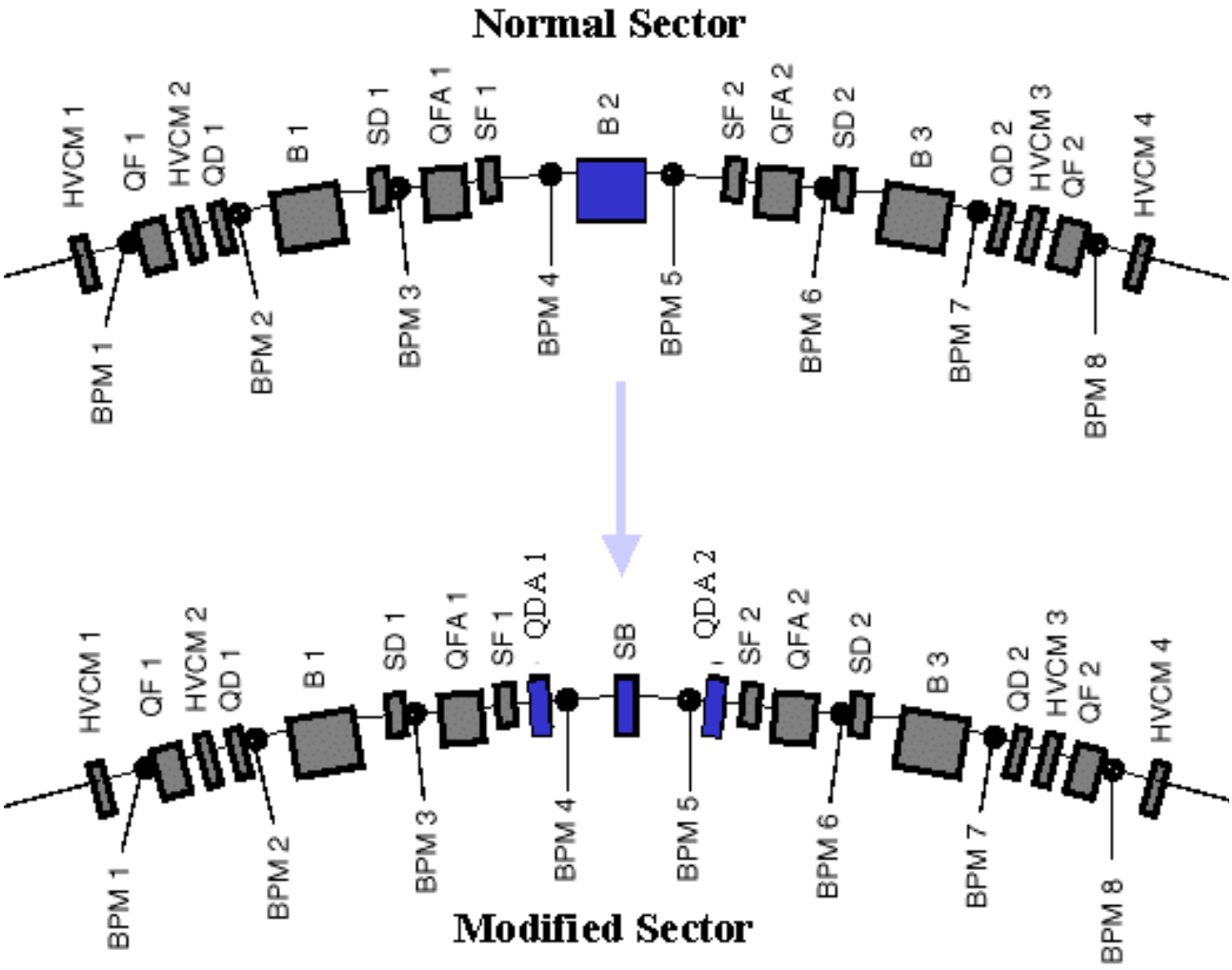

Fig. 3. Magnetic layout of a normal (top) and modified (bottom) sector.

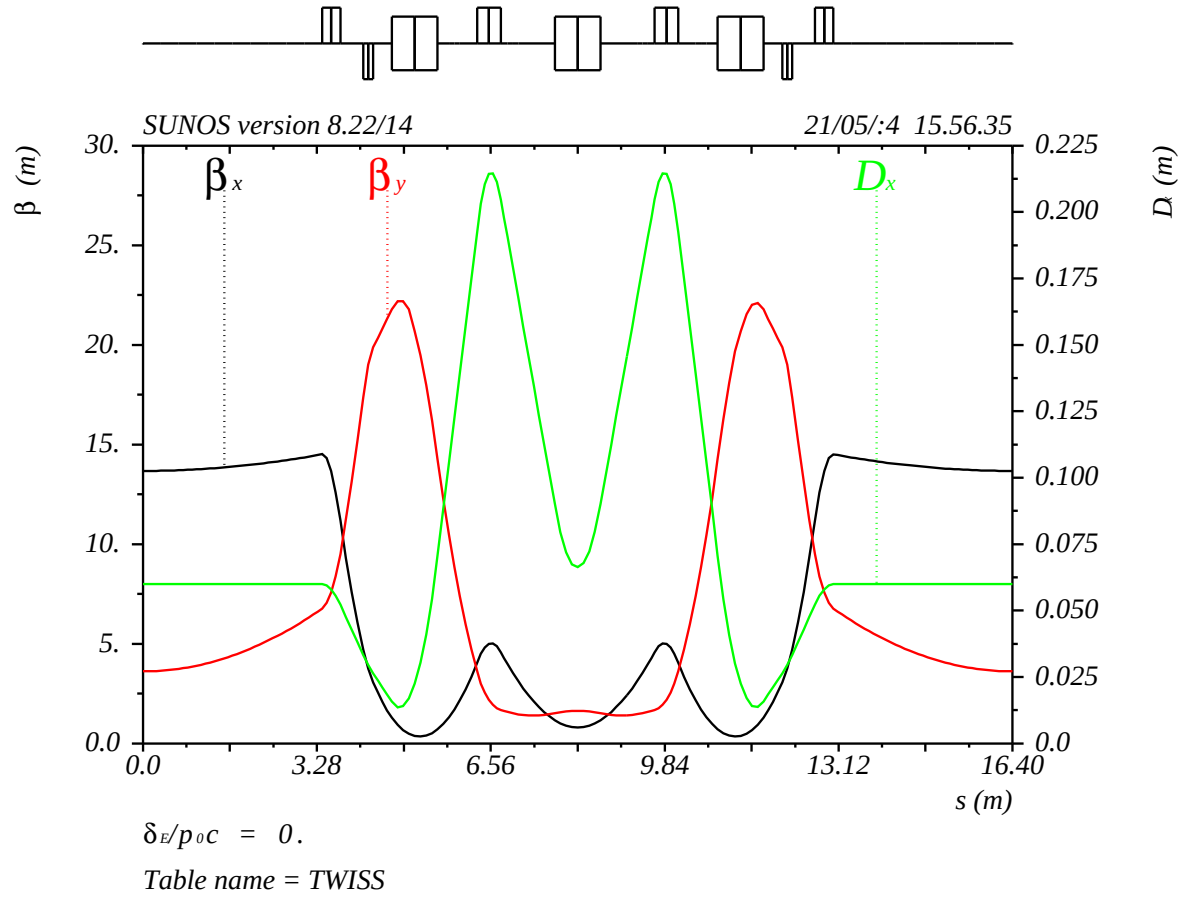

Fig. 4. Lattice functions $(\beta_x, \beta_y, \eta_x)$ of the ALS for the zero dispersion lattice used before Superbends were installed.

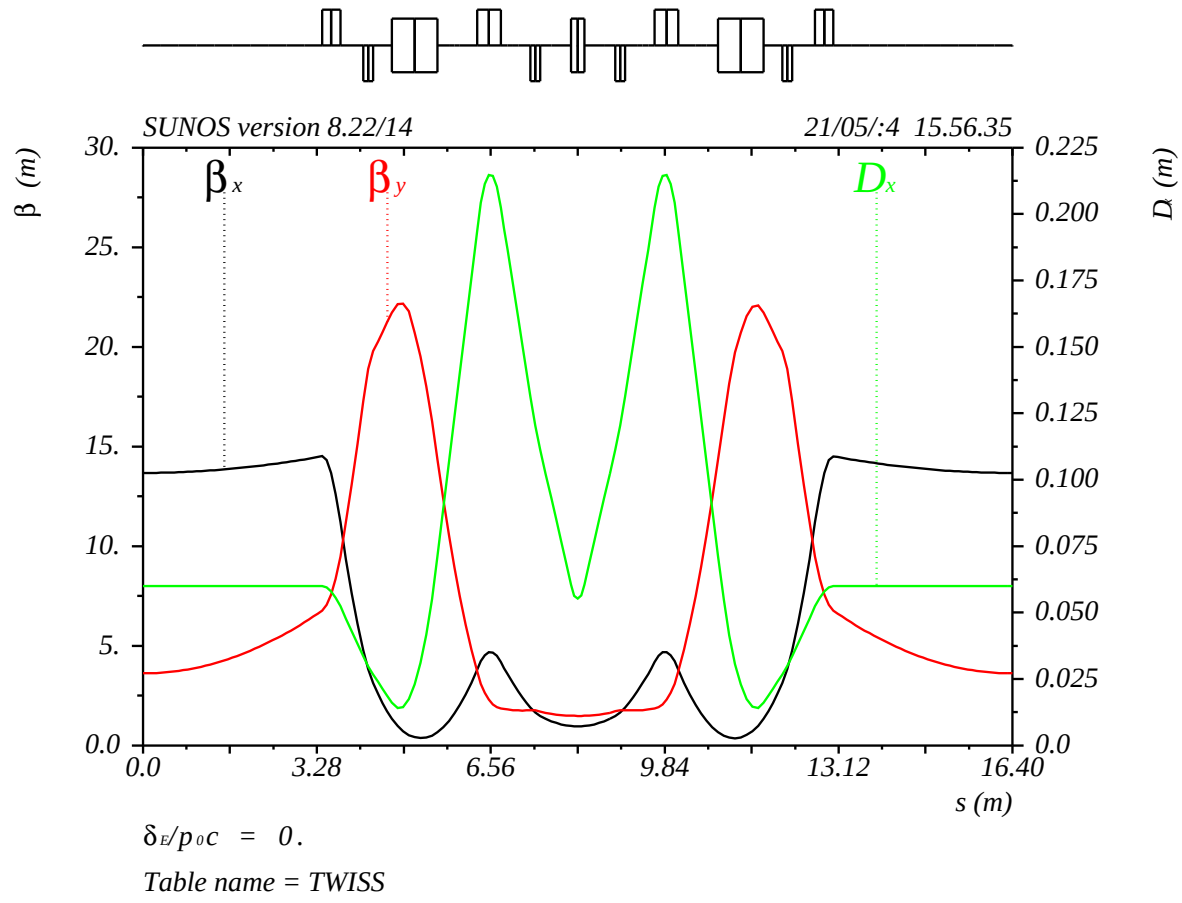

Fig. 5. Lattice functions $(\beta_x, \beta_y, \eta_x)$ of the ALS for the distributed dispersion lattice (6 cm horizontal dispersion in the straight sections). Shown is a sector with a Superbend magnet in the middle.

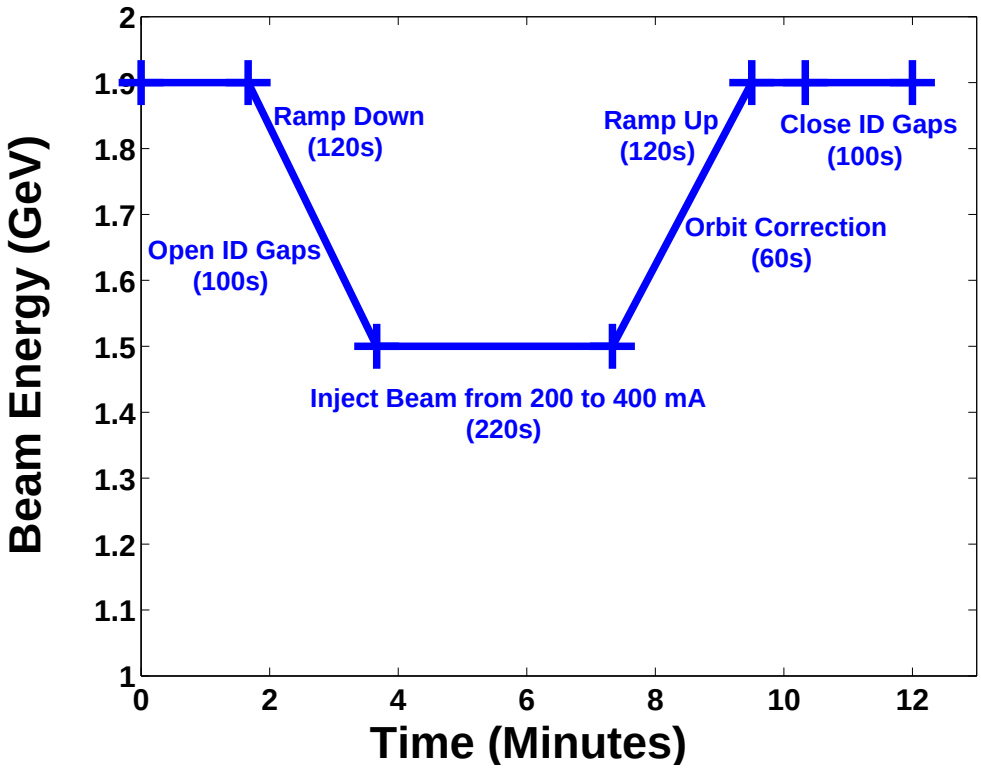

Fig. 6. Injection cycle before the Superbends were installed.

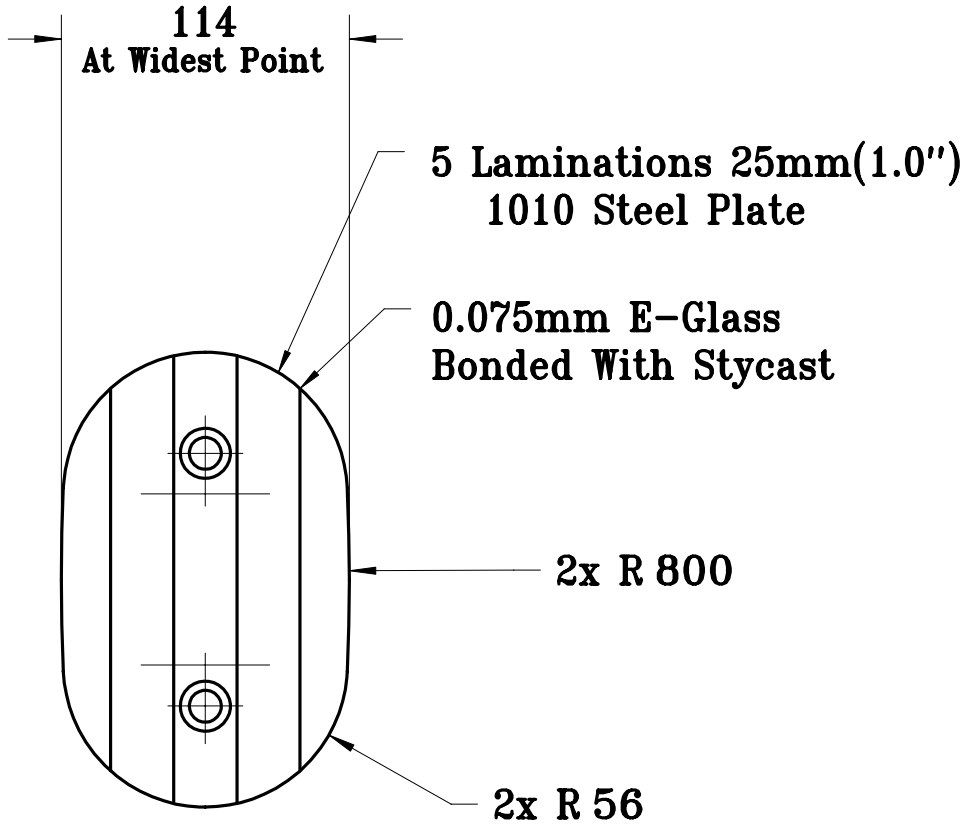

Fig. 7. Superbend magnet pole shape

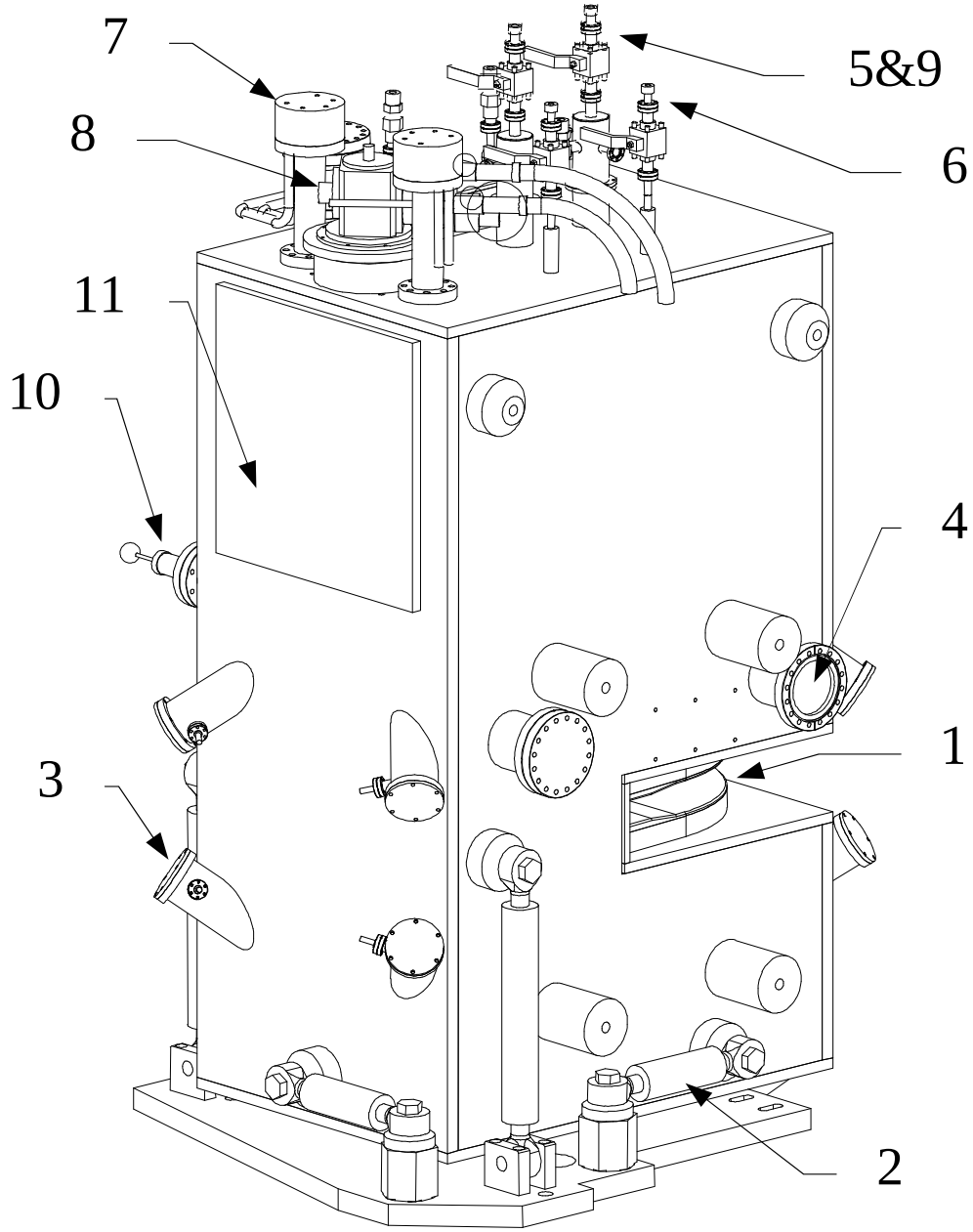

Fig. 8. Exterior configuration of the ALS Superbend: 1 - room temperature gap, 2 - suspension struts, 3 - cold mass suspension strap adjusters, 4 - cold mass fiducial viewport, 5 - LHe ports, 6 - LN_2 ports, 7 - current leads, 8 - cryocooler, 9 - rapid cooldown ports, 10 - rapid warmup feedthrough, 11 -access port.

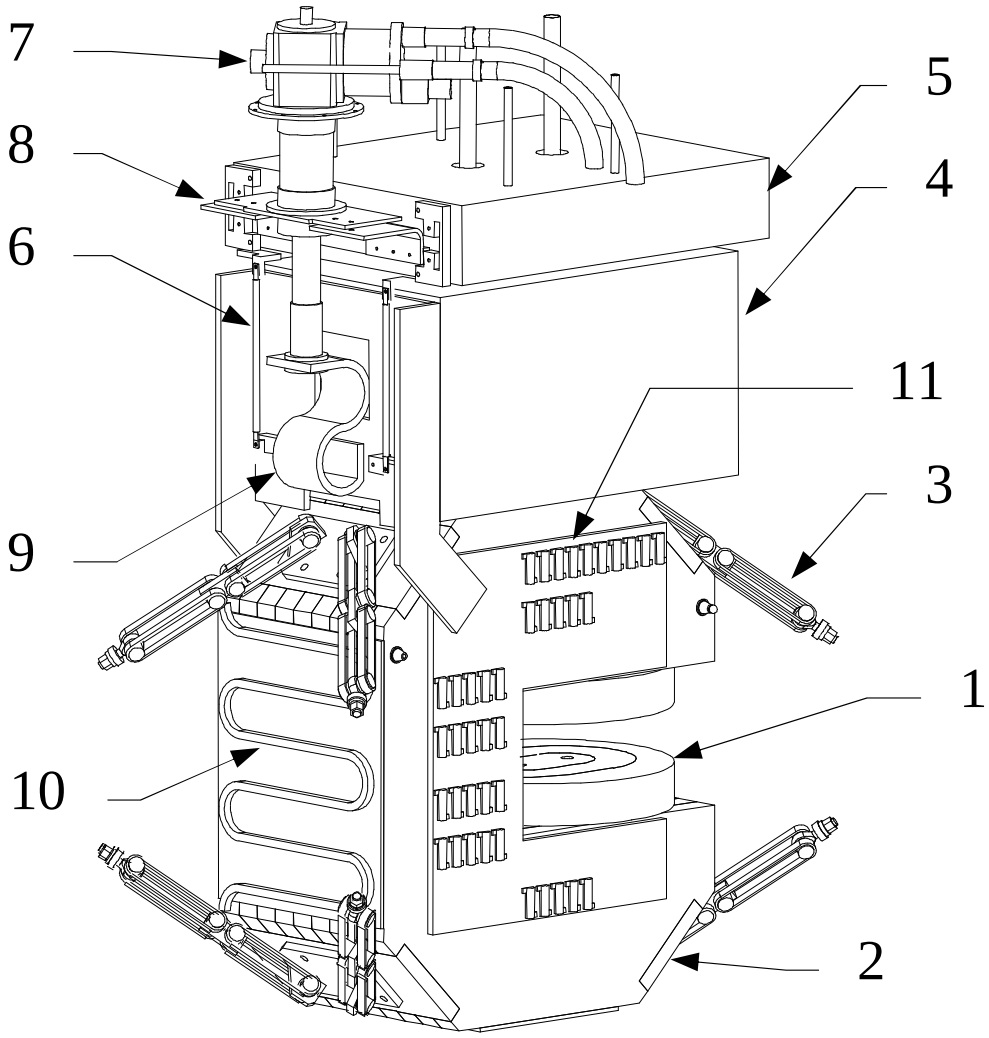

Fig. 9. Superbend cold mass assembly: 1 - superconducting coils with steel poles, 2 - laminated steel yoke, 3 - suspension straps, 4 - LHe vessel, 5 - LN_2 vessel, 6 - HTS leads, 7 - cryocooler, 8 - 50 K thermal connection, 9 - 4 K thermal connection (s-shaped link), 10- cooldown tube, 11 - warmup heater.

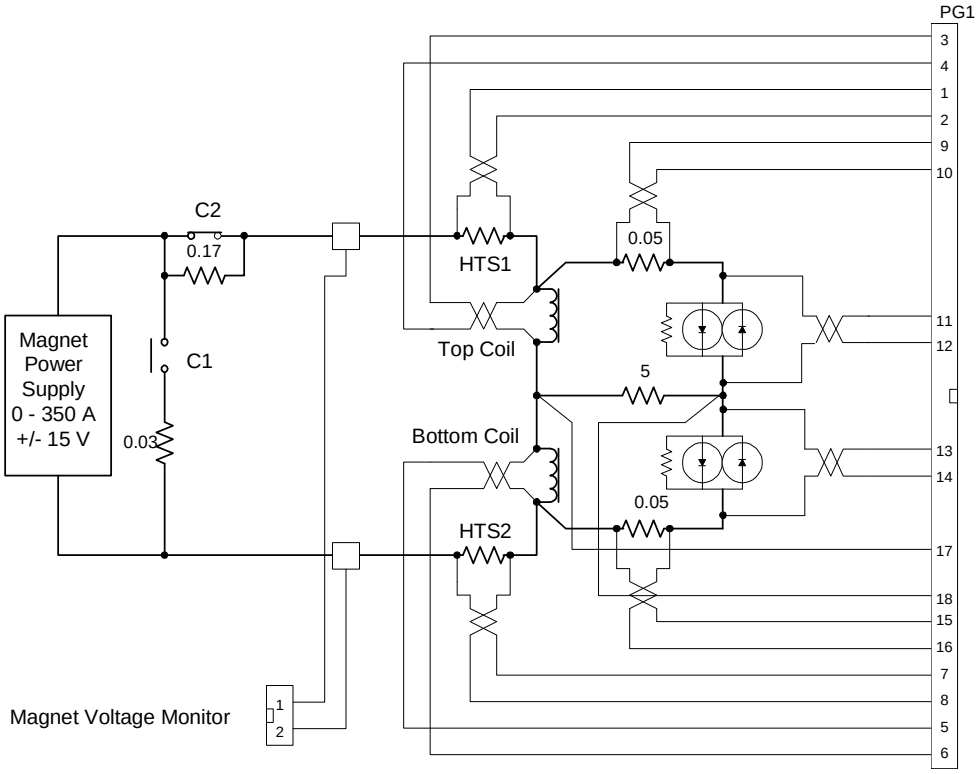

Fig. 10. Superbend power and instrumentation schematic.

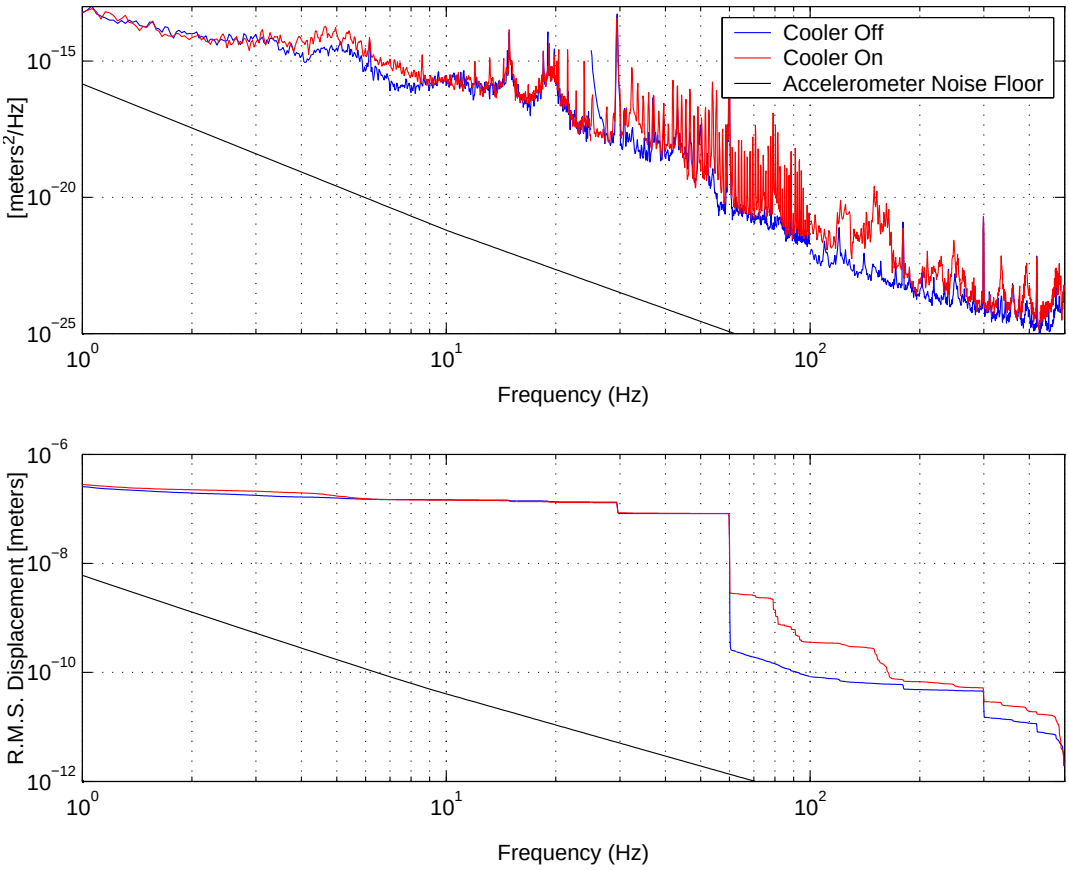

Fig. 11. Comparison of vertical vibrations of the cold mass (magnet yoke) with the cryo cooler on and off after the thermal connection between the cryo cooler and the cold mass had been optimized for minimum vibration transmission. With this modification the vibration induced by the cryocooler is significantly smaller than the tolerance of several microns (see Table 1).

Fig. 12. First Superbend magnet installed on the test stand.

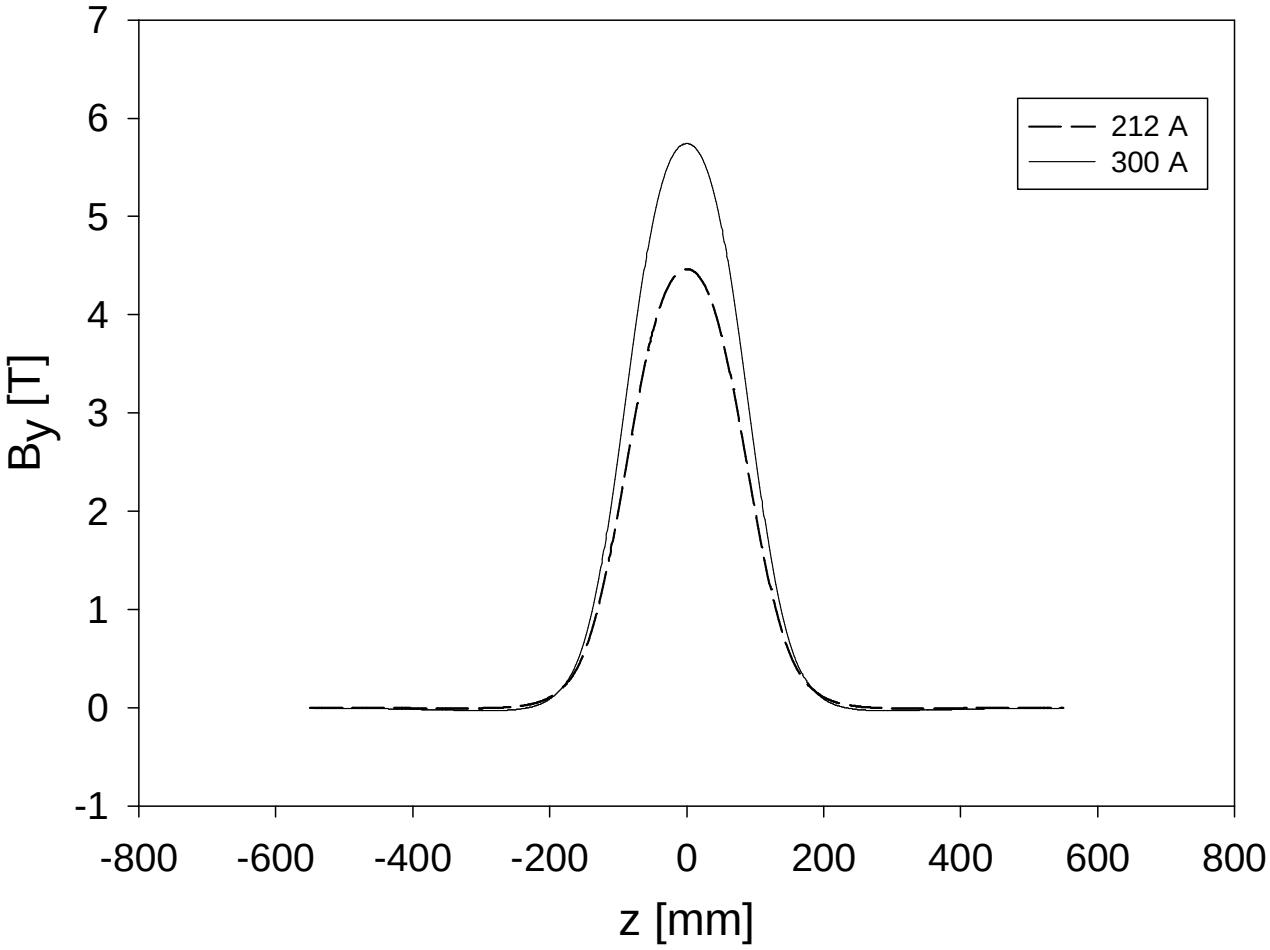

Fig. 13. Axial field profile of one of the Superbend magnets at 212 A and 300 A.

Fig. 14. The left photograph shows fixtures and tools used to machine the ALS aluminum vacuum chambers in situ, in preparation for the Superbend installation. The right photo shows the finished circular cut out for the Superbend cryostat.

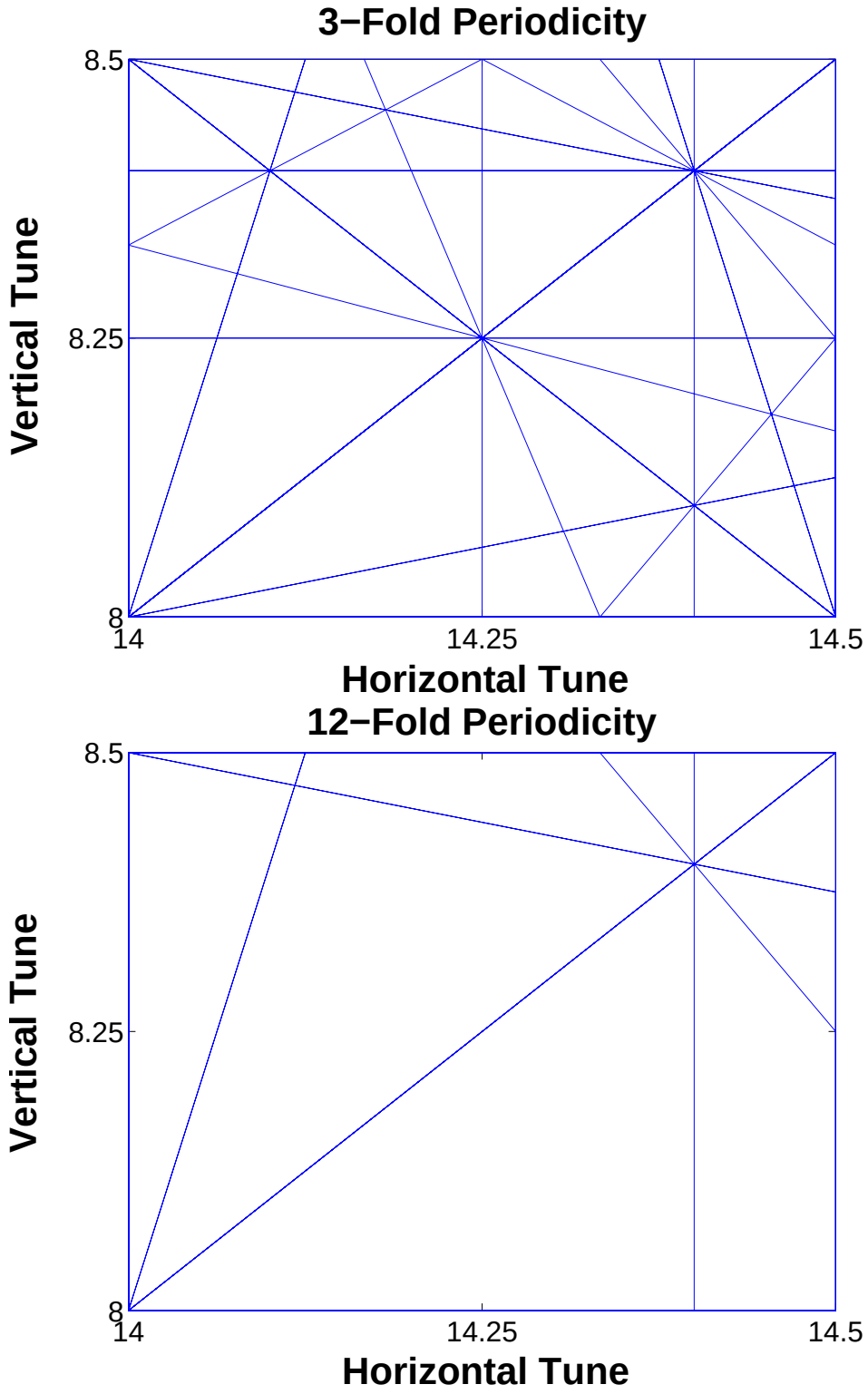

Fig. 15. Allowed resonance up to 5th order in the case of 3-fold periodicity (top) and 12-fold periodicity (bottom).

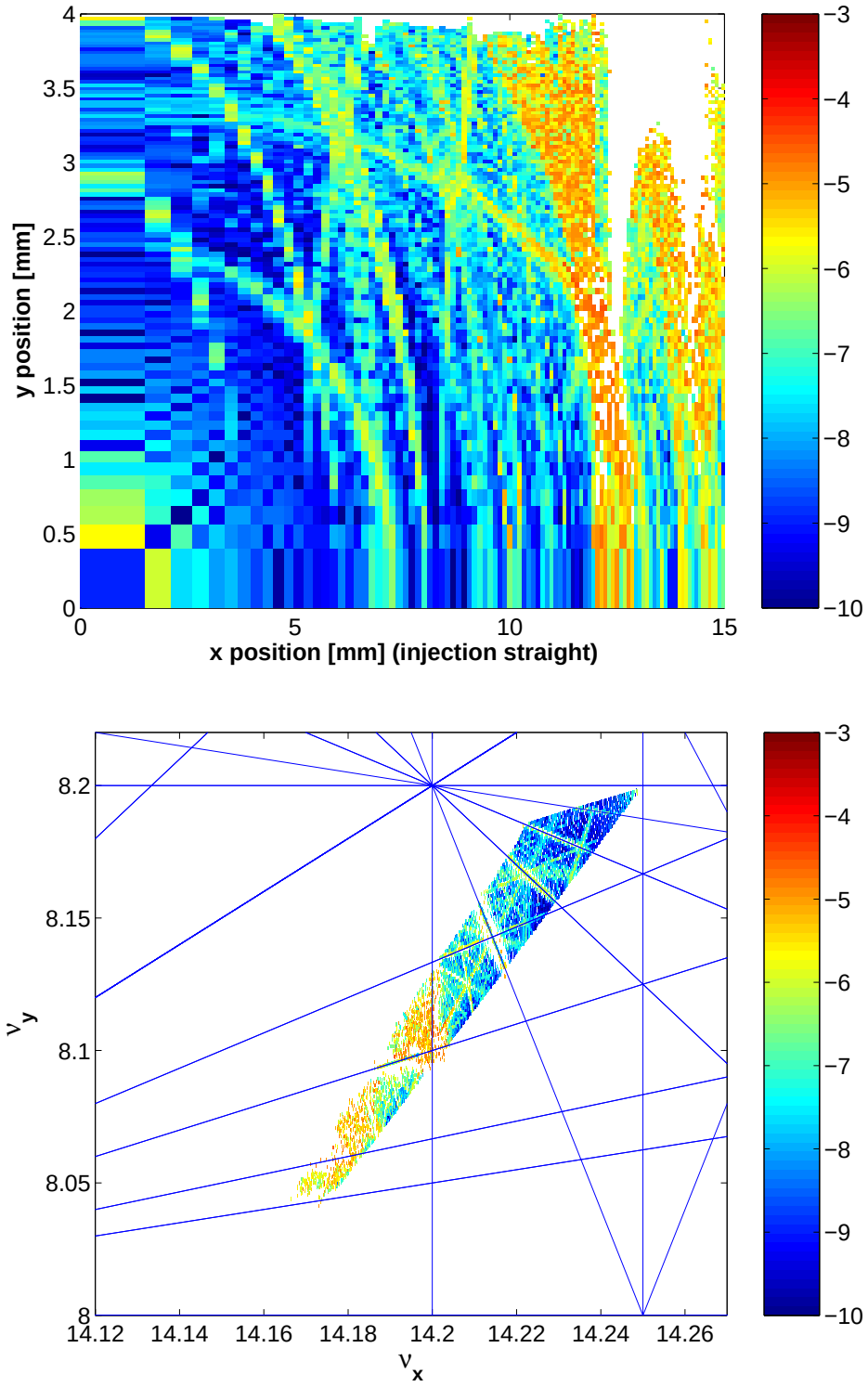

Fig. 16. On-energy frequency map of the ALS before Superbends with zero dispersion lattice plotted in tune and configuration space at the injection point.

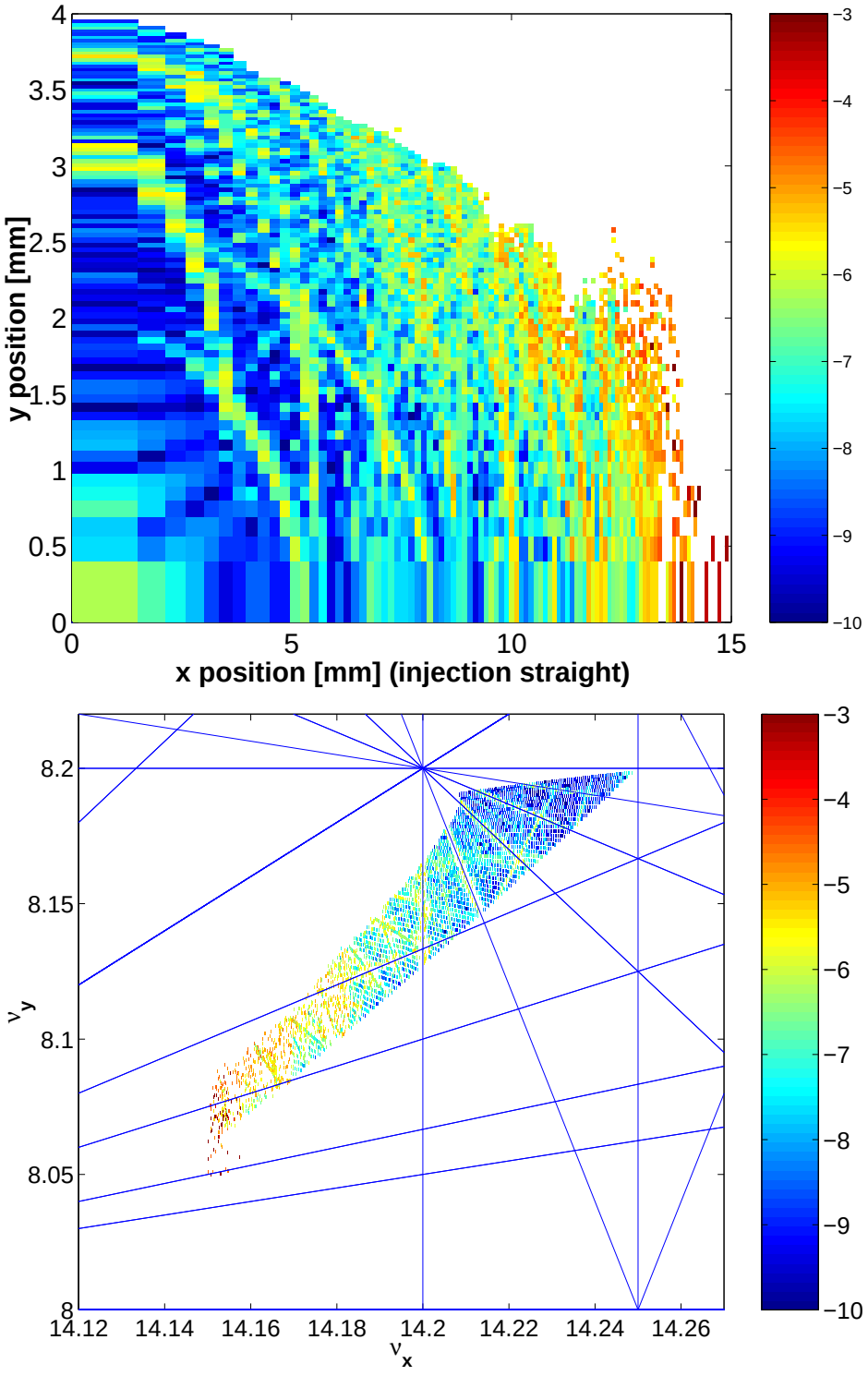

Fig. 17. On-energy frequency map of the ALS with three Superbends and the distrbuted dispersion lattice plotted in tune and configuration space at the injection point.

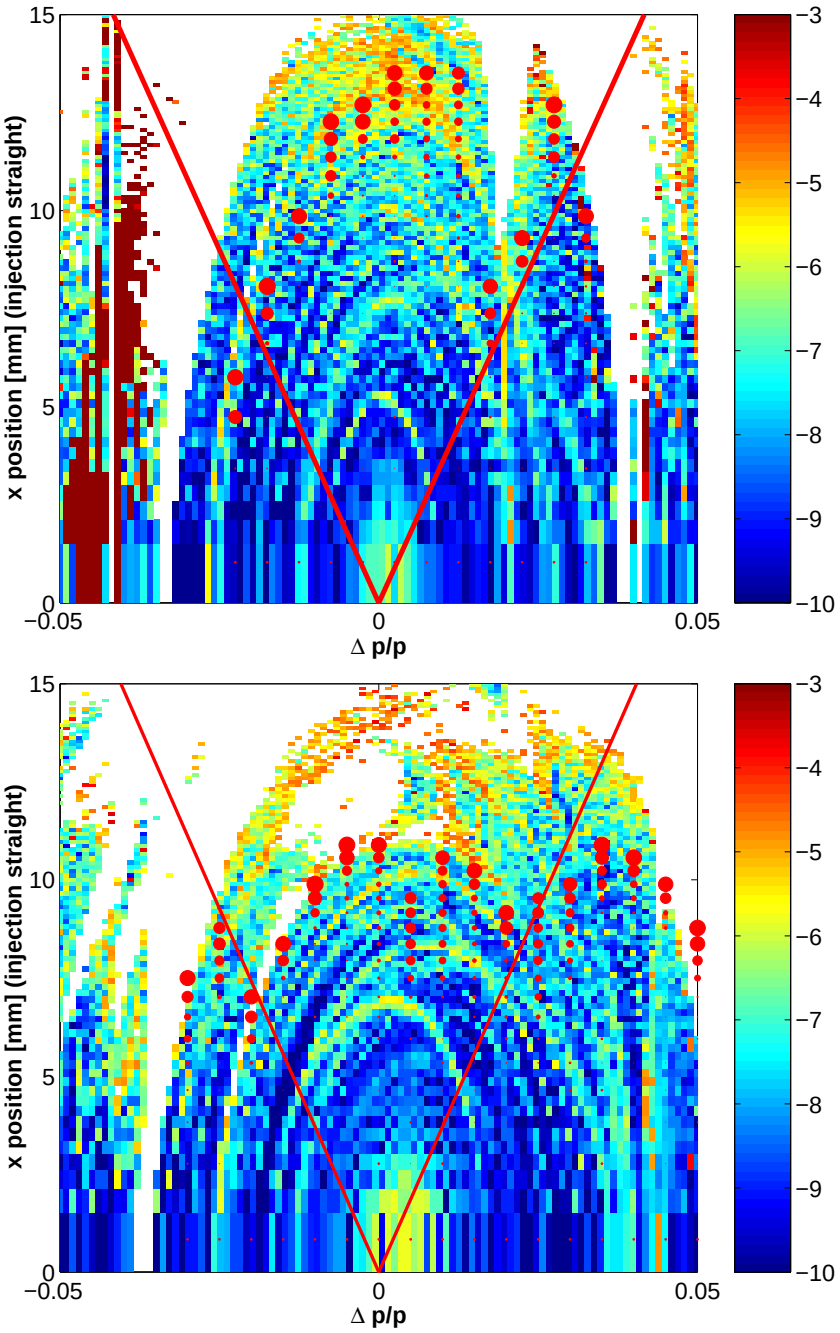

Fig. 18. Off-energy frequency map and measured off-energy dynamic aperture of the ALS for cases where the periodicity breaking due to one or three Superbends was simulated using the pre-installed quadrupoles next to the future Superbend locations. On the left is the case with three simulated Superbends and the distributed dispersion/lower emittance lattice. On the right is the case with only one simulated Superbend, i.e. a lattice periodicity of only one, and a zero dispersion lattice.

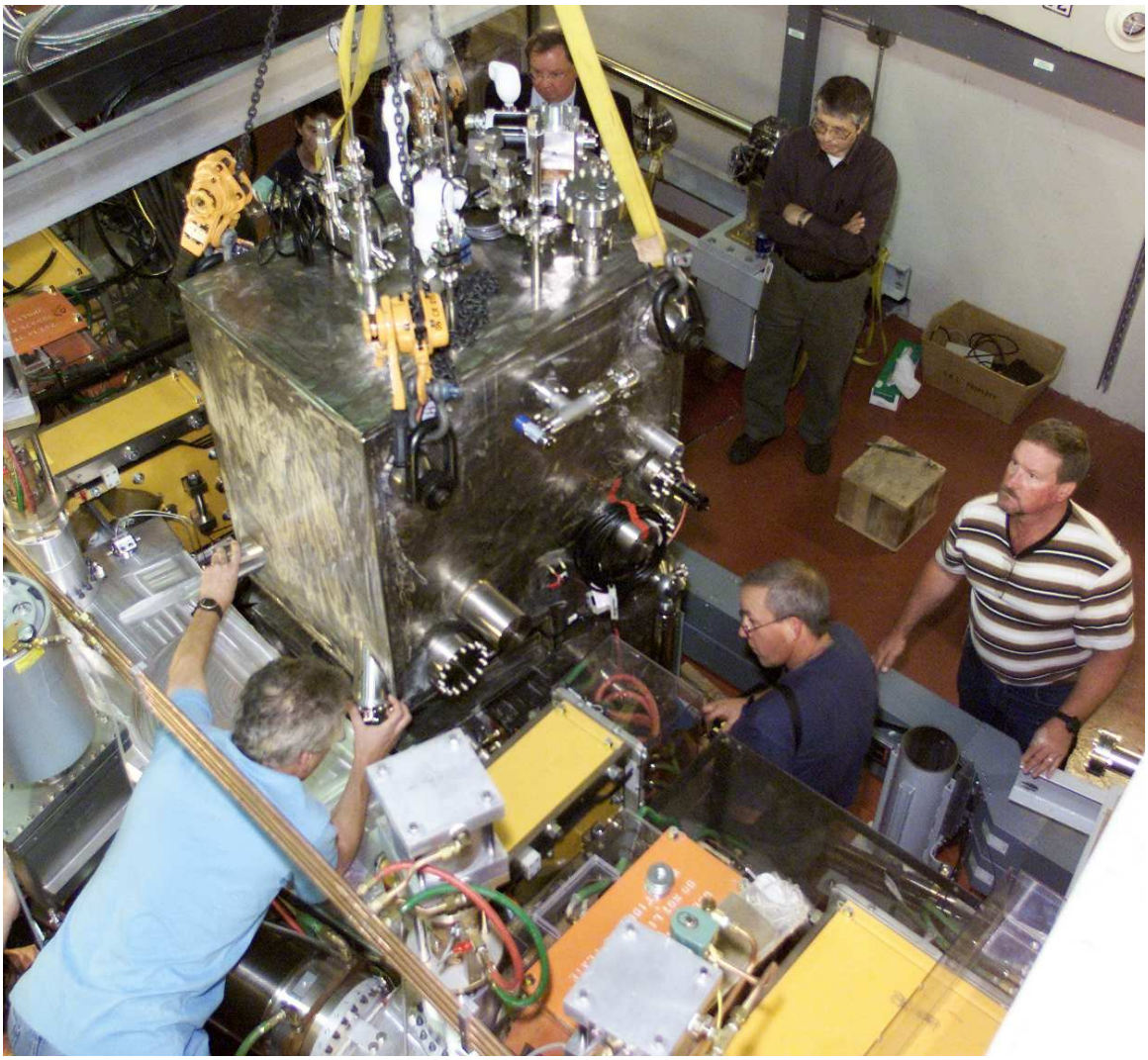

Fig. 19. Installation of the first Superbend.

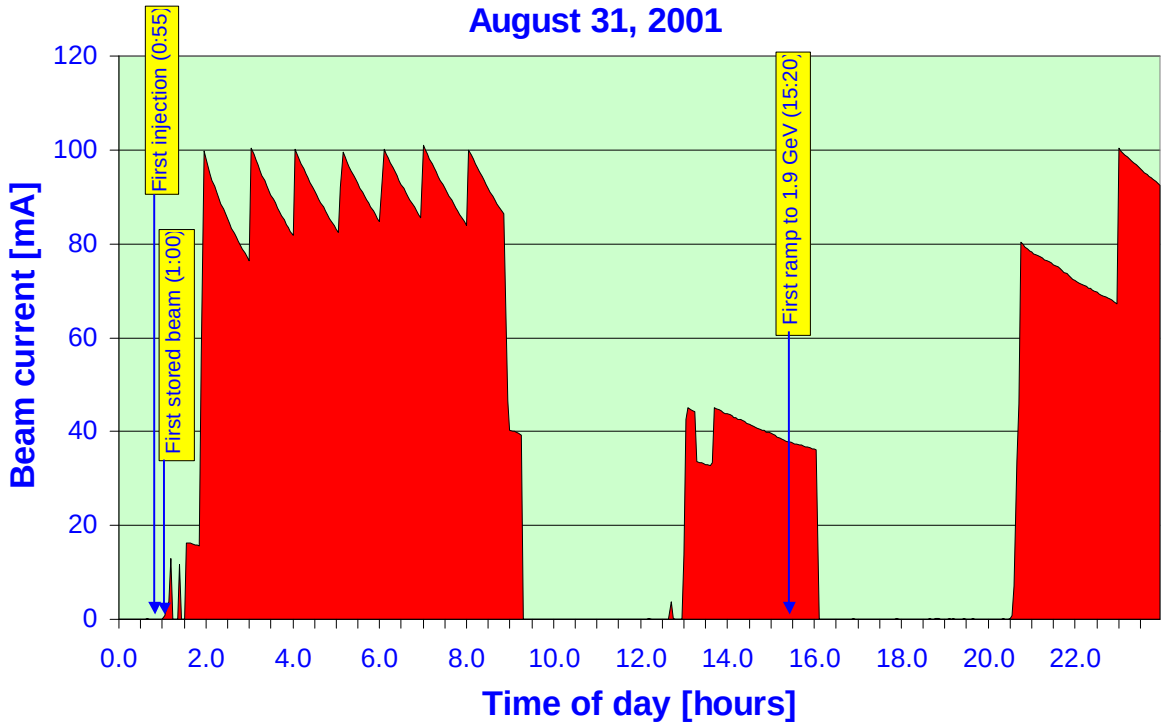

Fig. 20. Beam current history of the first commissioning day with Superbends. Some accomplishements are labeled on the plot.

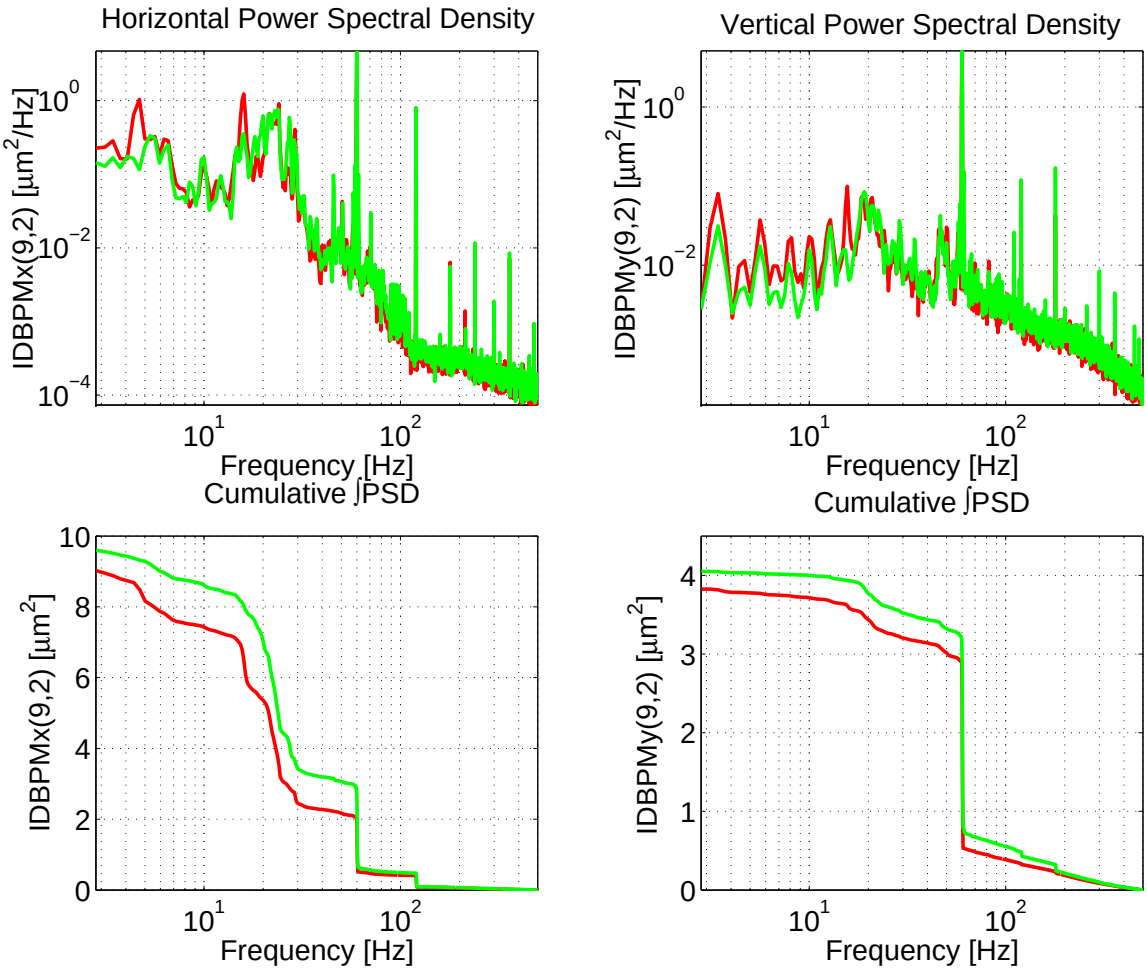

Fig. 21. Power spectral density of the closed orbit oscillations in the ALS before (red) and after (green) the installation of the Superbends.

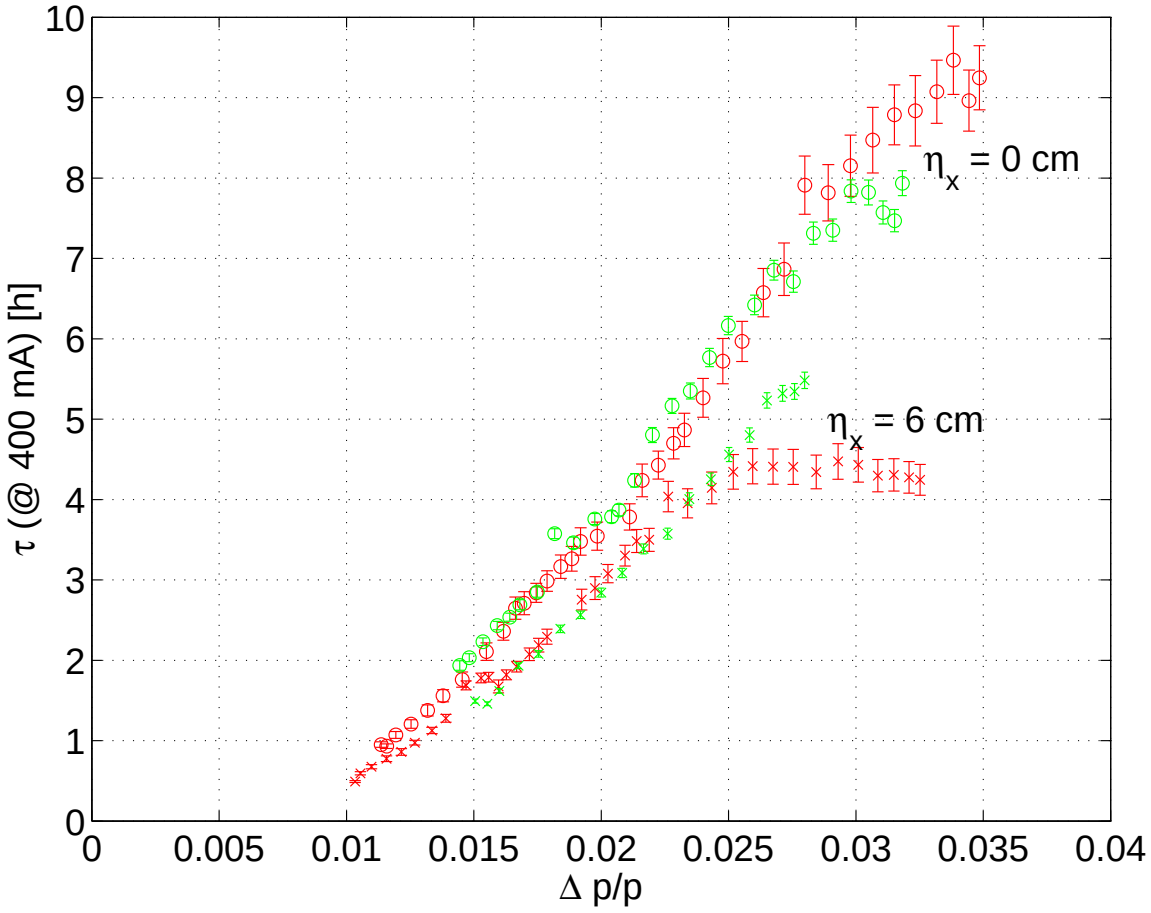

Fig. 22. RF aperture scans before (red) and after (green) the installation of the Superbends. The slightly different vertical scaling best visible in the rf-acceptance dominated areas is caused by the different emittances (bunch volumes) in the different lattices.

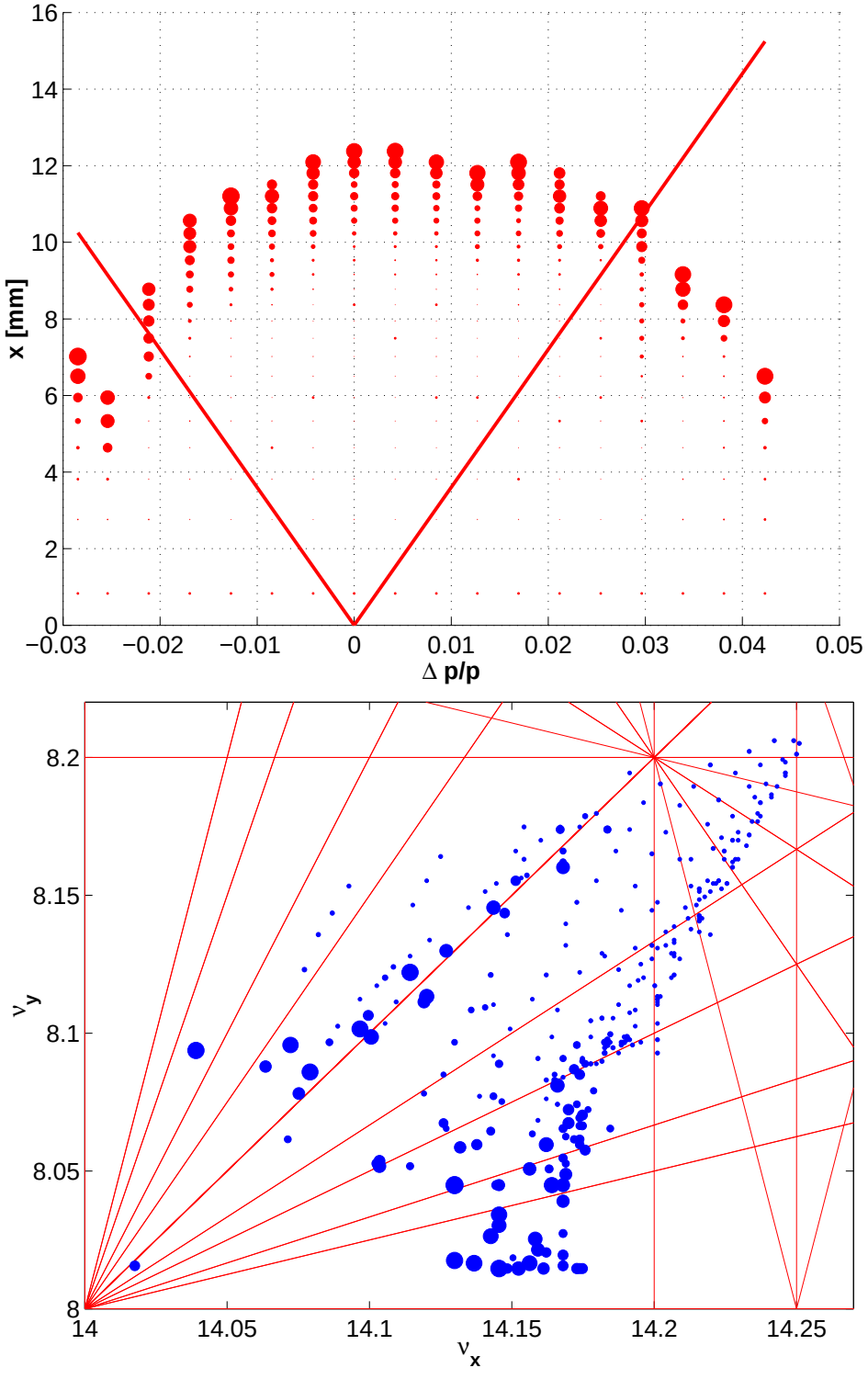

Fig. 23. Measured off-energy frequency map and off-energy dynamic aperture of the ALS with the distributed dispersion lattice and three Superbends.

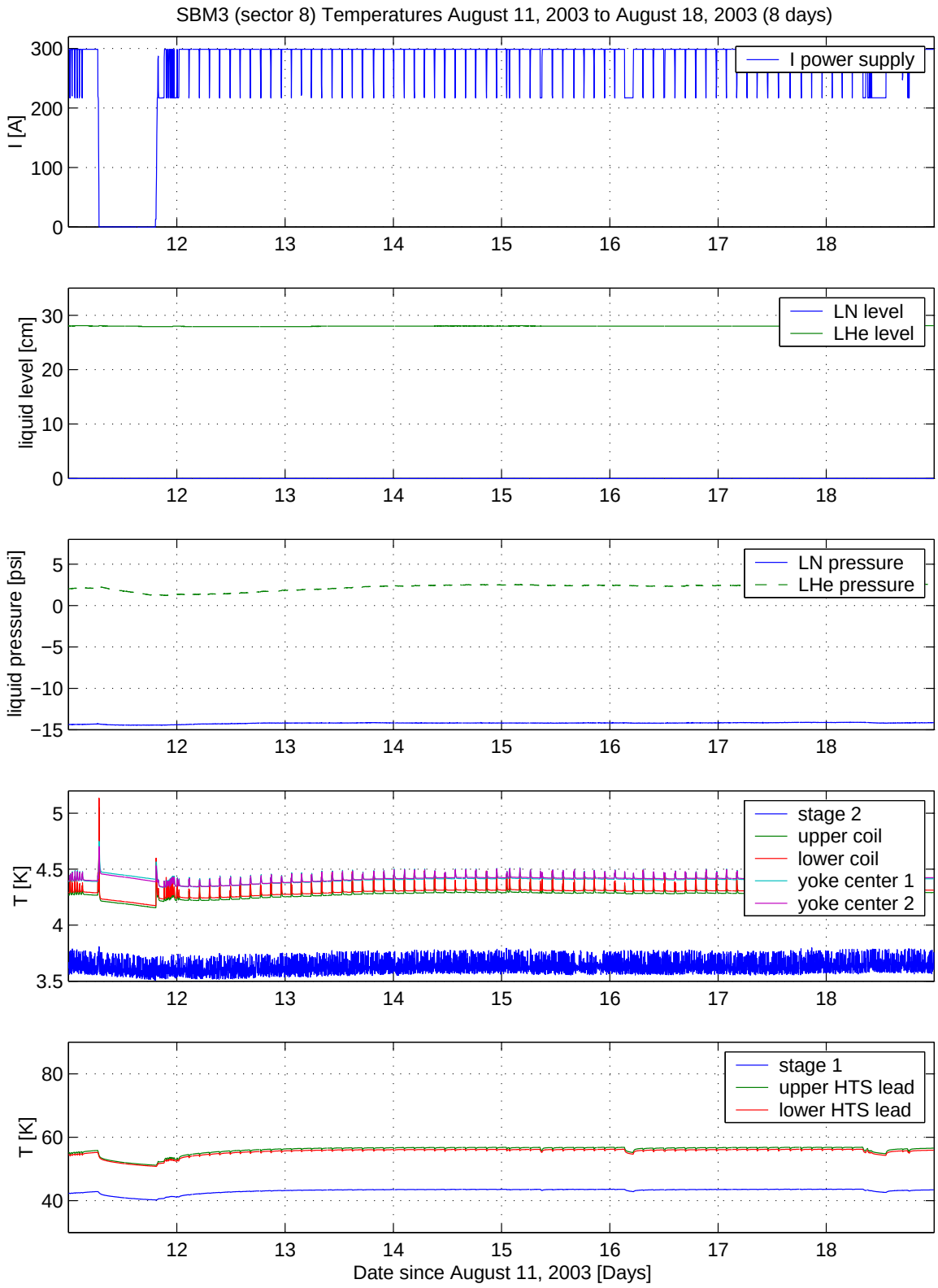

Fig. 24. Operating temperatures of the cold mass, magnet current and cryo system pressures of one Superbend magnet during one week of two bunch operation.

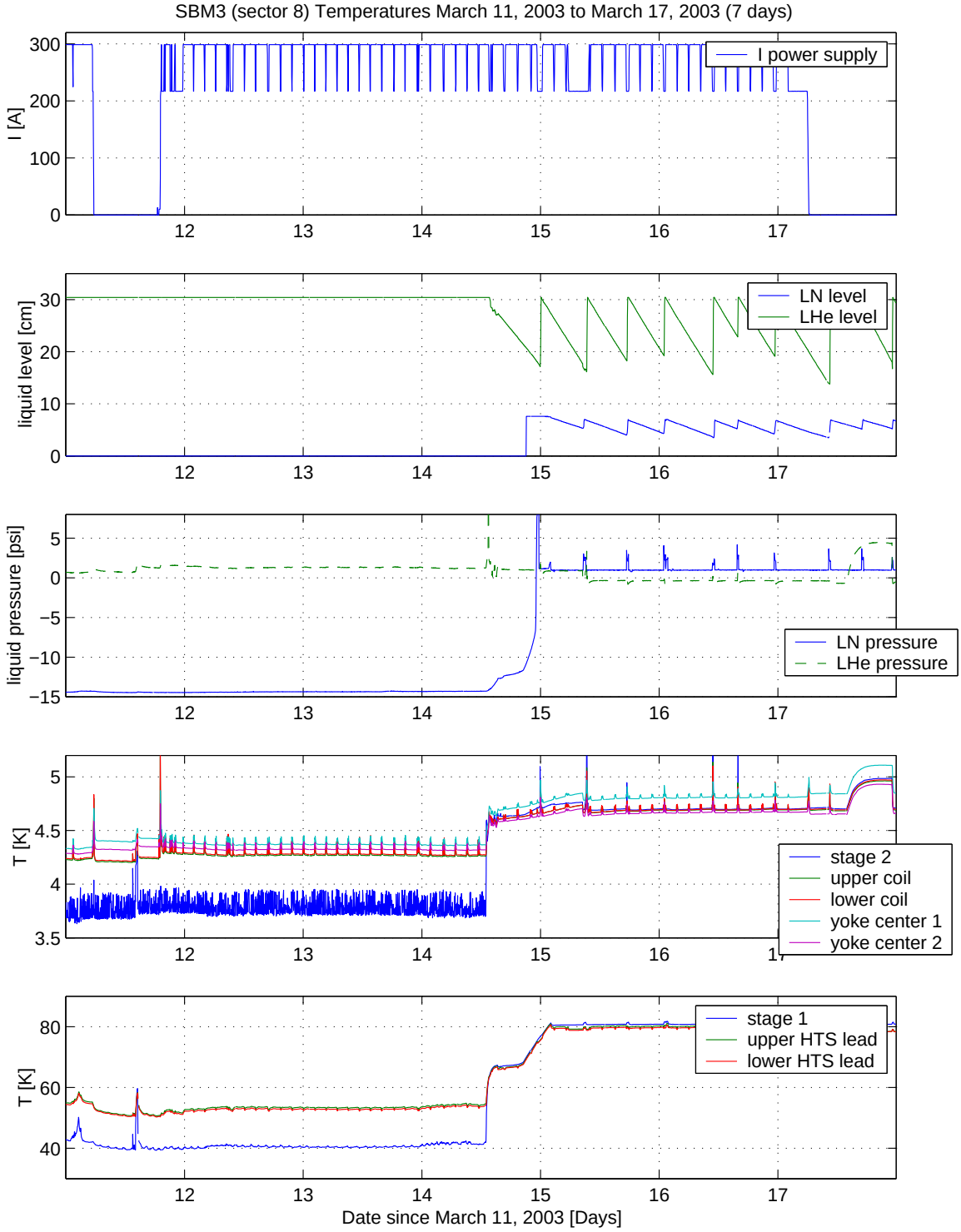

Fig. 25. Operating temperatures of the cold mass, magnet current and cryo system pressures of one Superbend magnet during and after the one cryo cooler failure in March 2003.